Transilvania
University
of Brasov

**INTERDISCIPLINARY DOCTORAL SCHOOL**

**Faculty of Technological Engineering and Industrial Management**

**Eng. Andrei – Ionuț BERARIU**

# Active control of vibrations induced by the cutting process in the machine tool structure to improve machining accuracy.

# Controlul activ al vibrațiilor induse de procesul de aşchiere în structura maşinilor-unelte în scopul creşterii preciziei de prelucrare

**SUMMARY**

**Scientific coordinator**
**Prof. Dr. Eng. Tudor – Ion DEACONESCU**

**BRAȘOV, 2023**

# Content

# 1 INTRODUCTION

Cutting operations are still the most common ways of surface generation used in the manufacturing industry, constantly evolving and diversifying. In most cases, the cutting processes are accompanied by dynamic phenomena that have a significant detrimental impact on surface quality and cutting tool durability. Monitoring these phenomena can be done using complex techniques for estimating and measuring the various physical quantities associated with the chip formation process and the dynamic stiffness state of the machine tool (MT).

Artificial intelligence (AI) is now one of the most intensely researched disciplines in computer science. Due to the large number of variables that can influence the occurrence of chatter phenomena, it is difficult, if not impossible, to develop quantitative analytical relationships/models capable of providing relevant information on the occurrence and control of this phenomenon. A possible alternative to this is the use of AI technologies. A major bottleneck in terms of implementing AI technologies in manufacturing is the training phase of the neural networks. In general, this stage of implementation requires a large number of samples, their availability and/or cost being one of the main drawbacks.

The thesis proposes a developing platform focused on implementing AI based systems into manufacturing centers in order to control the dynamic phenomena of cutting processes by using the latest finite element simulation methods (CAE/FEM) and parametric explorations solutions (DSE). The obtained sample set was used in the last part of the research, where several variants of neural networks were tested. The tests aimed to identify and expose the main building and training parameters that directly intervene on computational and prediction performance, with a focus on the complexity difference of the two train data sets ($Fx$ and $Fy$).

## 1.1 Purpose and objectives

The thesis is largely focused on the development of a complex platform for the implementation of artificial intelligence (AI) technologies in machine tools (MU), capable of detecting and controlling the occurrence of the self-vibration phenomenon. The primary purpose was to create, prototype, and validate the essential components needed to train neural networks in this environment utilizing concepts borrowed from the Digital Twin concept.

Based on the current state of the art of the mathematical apparatus and techniques used in the analysis of dynamic processes, presented in the first part of the thesis, the methods for detecting and controlling the phenomena of self-vibration during cutting operations are critically analyzed. Based on the conclusions, it was possible to outline the problem from a constructive, physical and mathematical perspective by exposing the interdimensional relationships and limitations on the basis of which the physical phenomenon in question can be approached. Using AI technologies implies performing a preliminary training process, which generally requires a large number of samples. The main objectives pursued in the thesis revolve around this critical stage by proposing synergistic approaches for the generation of these samples synthetically using the latest numerical techniques. Their generation involves decoupling the dynamic system into two critical components: the first component focuses on obtaining the forces induced by the chip formation process, and the other is the modal component of the complete system with which the disruptive source will engage. In order to obtain the first component, different estimation methods were explored, the final solution adopted being the use of finite element methods. A secondary objective resulting from the adoption of this solution is to optimize the computational efficiency by dimensional reduction of the numerical model used, while controlling the level of correlation. The scalability of the simulation method is ensured by means of a conversion solution, a solution that allows the application of the methodology of synthetic generation of dynamic samples on simple processes such as turning and on processes with a higher degree of complexity such as milling operations. In order to facilitate the effective exposure of the interdependencies of the parameters involved in the chip formation process, the number of possible combinations being very high, the use of modern parametric exploration methods was proposed. These methods have the ability to expose, through a reduced number of configurations, the main parameters of influence and the critical variation areas that might induce the appearance of harmonic vibrations during chip formation. The modal characteristic of the generator system can generally be determined experimentally or using various numerical estimation methods. The finite element simulation method offers the most flexibility in exploring various process configurations, but this method cannot always be applied to all machine tools, especially old ones. The availability of geometric and physical information is the main impediment to the use of these methods. Consequently, the present work focused on the development of an experimental system capable of measuring the transfer functions (accelerance, inertance) of the tool-tip. The objectives pursued in this stage are aimed at the development of the pretensioning devices of the generator system without interfering with the modal behavior. Advanced optimization techniques and parametric exploration were used here also that allowed the creation of the final measuring devices used to map the dynamic stiffness values on a physical CNC lathe, values subsequently coupled with the load spectra. In the final part of the work, different configurations of neural networks were explored, evaluated and proposed in order to estimate the states of dynamic stability for cutting processes. Essentially, the main objective was to expose the complexity of the training process and how both the number of samples and the hyper-parameters used can influence the final performances. A critical aspect resulting from this last stage of validation is that related to the trainning cost, an acceptable reaction speed of such a feedback loop system being strongly influenced by this aspect.

## 2.2 Dynamic stability of cutting processes

Depending on the values of the dynamic stiffness of the components of the mechanical cutting system (cutting tool, tool holder, clamping system, workpiece, etc.), three types of vibrations can be distinguished [27]:

a) Free vibrations;
b) Forced vibrations;
c) Self-Excited vibrations (chatter).

In the case of free and forced vibrations, it is sufficient to determine the sources to correct or mitigate their negative effects. Direct interventions on the cutting regime or in the MU structure have scalable and immediate effects, with little chance of failure (analytical / kinematic modelling, elimination of non-conforming components from the cutting system).

Self – excited vibrations are caused by periodic variation of the cutting forces produced by the interaction between the cutting tool and the workpiece. This type of vibration increases the instability of the system and leads to an increase effort to control the cutting regime. Depending on the dynamics of the generator system, three components of self – excited vibrations can be distinguished [27]:

1. Friction component;
2. Modal component;
3. Regenerative component.

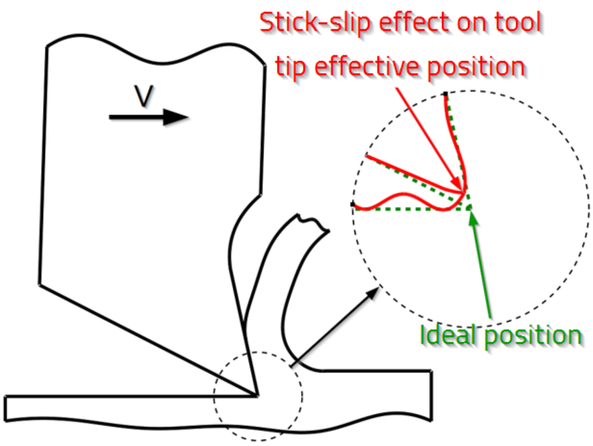


*Fig. 2.22 The effect of friction during turning (stick-slip)*

The literature exposes self-vibrations caused by friction and regenerative ones as being predominant in the appearance of unwanted vibrations ( chatter ) in the cutting processes [28]. This hypothesis is relatively recent and still requires a lot of research to be accepted. Other works propose as main contributors modal and regenerative self-vibrations [29]. Friction-induced self-vibrations (Fig. 2.22) are associated to the nonlinear cutting contact and the speed-dependent cutting forces. This particular case is called " stick-slip " which exponentially amplifies the system disturbances which can be compared to the resonance phenomena [27] [28].

Modal self-vibrations or modal coupling represent the phenomenon by which two or more natural modes of vibration, close in frequency but in different directions, enter a cumulation process [27] [28].

Regenerative self-vibrations (Fig. 2.24) are caused by the chip formation process and generation kinematics. During the cutting process, the cutting tool (or more precisely the active part) dislodges sections of material that have at least one face generated by the previous pass. This face prints the instantaneous dynamic behavior of the mechanical system leading to the variation of the thickness of the section to be dislodged. The kinematics is the main influencing factor in this case. The spatial complexity of chip generation is directly proportional to the number of dimensions in which this phenomenon must be modeled (if we compare turning and milling operations, milling is often more difficult to model/control in terms of regenerative self-vibrations) [27] [29].

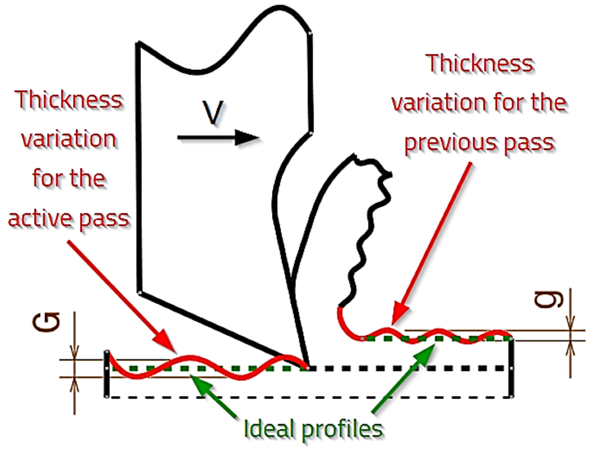


*Fig. 2.24 Regenerative vibrations caused by the variation of the chip section (g – previous; G – active pass)*

From this point, the present thesis focuses on turning and milling operations only beeing the most common used in practice for machining. It can be observed that in recent years the number of publications focused on the control of the self-vibration phenomenon in the MUs has dropped precipitously (Fig. 2.25), signaling the appearance of a theoretical limit and/or technical dept. History says that these periods of stagnation are caused by the different developing speeds that the research fields involved have [27].

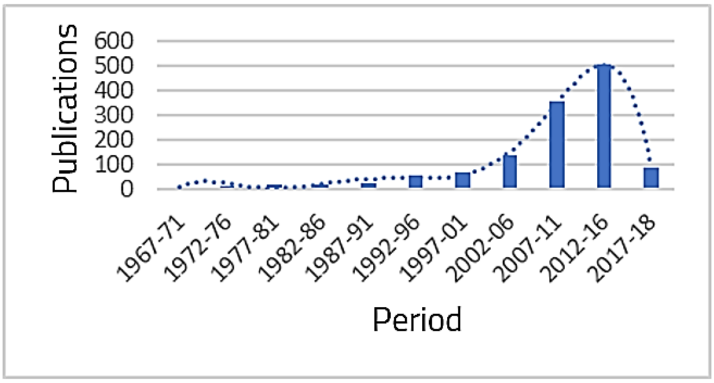


*Fig. 2.25 Research evolution for the self-excited vibration phenomena in milling operations [27]*

## 2.5 Conclusions

Usually, estimating the dynamic stability is the first step by which useful information related to the behavior of the entire generating system can be extracted. Most of the classical methods used for this purpose involve the separation of the two main active components in chip forming models and MU stiffness estimation models. Analytical techniques such as stability lobe diagrams or Nyquist diagrams have been and continue to be the main tools of analysis even in the context of aggressive digitization that all industries go through or have passed through (Industry 4.0).

In this thesis some common methods by which analytical determinations can be applied for turning and milling operations have been set forth. The main components involved in the analytical estimation of the dynamic stability of MU are: the cutting forces coeficients, the dynamic system parameters, the cutting process parameters and the cutting tool geometry. An alternative to analytical methods for estimating dynamic stability in cutting processes is the use of numerical methods (finite element method analysis). The main components required to correctly model the deformation process are: discretization, material modeling, friction modeling, and chip separation modeling. All these components are constantly being improved by private companies and researchers, and current trends suggest an attempt to unify and automate them.

The cutting processes have a suite of dynamic phenomena in their composition, each of which has the ability to influence more or less the precision of the operation. Vibrations are part of the category of the most important phenomena that must be studied and controlled (or avoided), because they have the ability to influence both the quality of the surface obtained and the durability of the cutting system and, in the extreme, can lead to the destruction of the entire generation system.

Currently there are several established methods of vibration measurement, mostly requiring contact with piezoelectric sensors. This method offers, in addition to the advantages of a development that began more than half a century ago, also the disadvantage of the fact that its development has reached the maximum possible given the physical limitations. For this reason, current research is focused more on the part of signal pre-processing and/or conditioning/filtering, trying to maximize the optimization of information obtained from sensors by means of computing systems.

If in the past the most expensive operation in the measurement chain was the storage and processing of the signals obtained from the sensors, nowadays this has become very accessible allowing the development of new digital means (acquisition systems and computer programs) capable of filtering, processing and extracting a wide range of information with relatively high precision given by complex mathematical algorithms impossible (or inaccessible) to execute in the past.

In parallel with the development of the sensors went also the mathematical modeling of the vibrating phenomenon, this aspect being strongly correlated with the new developments in computing power. The development of a high-performance vibration measurement and / or control system for MUs involves research of both branches. New methods of trying to capitalize on original mathematical models are continuously developed and show promising results, suggesting a possible return to the subject in future research.

# 3 THEORETICAL AND EXPERIMENTAL STUDIES ON ACTIVE VIBRATION CONTROL IN MACHINE TOOLS

The continuous development of sensors and processing technologies allows the advancement of methods and systems used for measuring cutting forces, often accompanied by specific sound signals, which allows the detection of stable or unstable regimes [88].

*Table 3.1 Setups used for chatter detection [89]*

| *Operation* | *Physical quantity* | *Sensor* | *Signal processing type* | *Chatter detection criterion* |
|---|---|---|---|---|
| *Milling* | Sound emission | Microphone | PSD | Energy levels |
| *Turning* | Vibrations | Accelerometers | Cross coherence | Coherence trend |
| *Milling* | Vibrations + Cutting Forces | Eddy sensors<br>Dynomometer | PSD | Qualitative analysis |
| *Milling* | Vibrations | Laser | Tool trajectory | Qualitative analysis |
| *Turning* | Cutting Forces | Dynomometer | CER | Qualitative analysis |
| *Milling* | Sound emission | Microphone | OPRS | Threshold |
| *Milling* | Cutting Forces | Dynomometer | WT | Threshold |
| *Milling* | Vibrations | Eddy sensors | OPRS, PS, PSD | Threshold |
| *Grinding* | Sound emission + Cutting Forces | Eddy sensors + Microphone | Entropy | Threshold |
| *Milling* | Sound emission + Cutting Forces | Dynomometer + Microphone | PSD | Threshold |
| *Milling* | Cutting Forces | Dynomometer | FFT | Distribution of spectral peaks |
| *Milling* | Vibrations | Laser | OPRS, PS, PSD | Threshold |
| *Milling* | Sound emission | Microphone | PSD | Threshold |

Table 3.2 illustrates some recent detection systems, organized according to the cutting operation, the physical quantity measured, the type of sensor, the signal processing technique and the detection criterion used. Both the frequency band used and the sensor positioning play a crucial role in correctly identifying this phenomenon. An appropriate frequency band for this type of measurement is between 100 and 5000 [ Hz ].

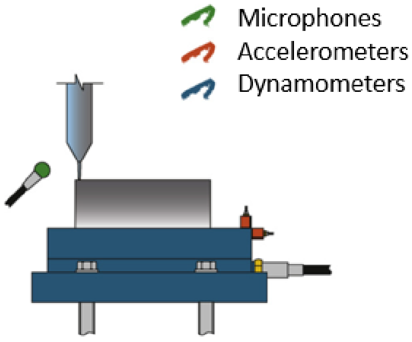


*Fig. 3.16 Usual sensor arrangement [90]*

A general rule regarding sensor positioning is to be as close to the source as possible, but this is not always possible [ 89 ]. According to recent research, the most recommended sensors for milling operations are accelerometers, dynamometers and microphones ( Fig. 3.16 ). There are also cases where other sensors are more efficient, such as Eddy or laser sensors, but their positioning is difficult, especially for machine tools with complex kinematics. At the same time, dynamometers also have important limitations such as the maximum working band which is somewhere around 1 [ kHz ]. Microphones have many advantages, such as high accuracy and low cost, but require a controlled operating environment due to the many noise-disrupting sources that can occur around the machine tool.

## 3.4 Conclusions

The first step to be taken in order to control self-excited vibrations (chatter) phenomena is their detection. Commonly, we can distinct the various types of detection methods based on cutting operation, measured physical quantity, sensor/s, type of signal processing and detection criterion. For turning monitoring, it is usually recommended to use accelerometers and spectral analysis of the signals. For the milling operations, the methods are a bit more complex commonly monitoring acoustic emissions and cutting forces through microphones and dynamometers respectively. In an attempt to unify the proposed solution/s, the thesis will use the common monitoring method in both turning and milling operations.

The first vibration control devices were passive. Passive control is generally applied to machine tools by means of filters, but in general this control can also be achieved by means of a machine tool design optimization. The domain of the devices (absorbents) used to control cutting processes is quite limited. However, it should be noted that each type of absorber is capable of handling a certain type of excitation and reacts on predetermined frequencies with limited possibility of adjustment.

Active vibration control systems in machine tools are being treated with great interest by the scientific and industrial community due to the multiple advantages they can bring. The first is the ability to continuously adjust the damping through the direct control of the cutting parameters or, indirectly, through the adjustments of the physical attenuation systems. If for passive approaches the dynamic model must be known in advance, in the case of active methods it can be determined experimentally by means of open or closed-loop systems. A unification of control models is thus possible which will ultimately lead to increased flexibility in their applicability.

# 4 EXPERIMENTAL STUDIES ON ACTIVE VIBRATION CONTROL IN MACHINE TOOLS USING ARTIFICIAL INTELLIGENCE

## 4.2 Monitoring/control of cutting processes using AI

The accelerated digitization movement (Industry 4.0) focused mainly on increasing productivity, reducing production costs and scrap has led to the emergence of automatic manufacturing centers. The systems have a multitude of automatic functions such as collision detection, process monitoring and certain types of optimizations. Most online optimization technologies ( even offline ) of the cutting process require a minimum level of measurement of dynamic signals. As a consequence, the identification and detection of self- excited vibration phenomena are topics often addressed by the scientific community. Based on what was discussed in Chapter. 3.1, it can be concluded that for the detection of the self-excited phenomenon in the cutting processes, measurements of cutting forces, accelerations, acoustic emissions or other electrical signals carrying characteristic information are used. These measured signals are evaluated in practice using various processing algorithms such as: Short-Term Fourier Transform ( STFT ), Wavelet Transform ( WT ), Wavelet Packet Decomposition ( WPD ), Hilbert-Huang Transform ( HHT ), empirical mode decomposition ( EMD ), Variational Mode Decomposition ( VMD ) or Local Mean. At the fundamental level, these self- excited vibration detection systems must perform three basic steps: collecting dynamic signals, extracting dynamic features from the signal, and evaluating the dynamic state of the system. Practically, the information generated by the last step can become input data for any passive (Chapter. 3.2) or active (Chapter. 3.3) control system, the collection of data (input + output) can be further used for the development of a digital twin model very useful for other more advanced applications.

The use of artificial intelligence in the detection/control of self-excited vibration phenomena in cutting introduces a new fundamental step, the training (and testing) of neural networks (see Chapter. 4.1). The data collection step aims to define as many sets of measurements as possible related to the state of the system. The use of a sufficiently large and representative set of samples in training the networks is essential for the generalization of the performance obtained in the end. Typically, for this type of application, the following types of neural networks are used: support vector machines (SVM), artificial neural networks (ANN), multilayer perceptron (MLP), unsupervised models, and DL-specific models such as convolutional networks (CNN).

Table 4.2 reports the performances obtained by the latest scientific research in the field of detection and/or control of the self- excited phenomenon in cutting operations. As can be seen, the scientific community is testing many configurations/techniques often combined with other more or less empirical methods, which have led to promising results. Most studies are performed in controlled environments, very different from normal operating conditions, while still using real cutting parameters to ensure the validity/scalability of the results obtained.

*Table 4.2 Performance reported in the most recent scientific studies related to the detection of self-excited vibration in machining [96]*

| Signal processing type | Model | Operation | Accuracy [%] |
|---|---|---|---|
| WT | MLP | Milling | 94 |
| WT | SVM | Turning | 95 |
| EMD | SVM | Turning | 95 |
| VMD | SVM | Milling | 92.59 |
| WT | CNN | Milling | 99 |
| STFT | CNN | Milling | 98.9 |
| EMD | AlexNet | Milling | 82 – 100 |

Unfortunately, it is still not possible to make a clear distinction between the performances obtained by advanced methods that use artificial intelligence and classical methods (those that monitor the vibration level by applying a simple RMS operation on the amplitude level) [96].

## 4.3 Synthetic generation of training samples

The main impediment in the implementation of technologies that use artificial intelligence is given by the large number of samples required by the training process. Ideally, the samples used for this process are generated experimentally because they can encompass all the features, known or hidden, leading to better accuracy of the predictions generated by the network. However, this is only possible for certain applications, such as facial recognition or handwriting recognition, because the nature of the samples is very common (pictures, songs, videos, etc).

The specifics of the addressed problem, vibration control of machine tools, directly shape the fundamental structure that a sample must possess. In order to ensure data compatibility, it is necessary that the information, both input and output, be composed coherently based on the phenomena/parameters to be modeled by the neural network.

The input data of this tensor is represented by the physical, dynamic and geometric characteristics of the monitored/controlled process. In the case of machining, these are: the material/physical properties of the workpiece, the material/physical properties of the cutting tool, the parameters of the cutting regime, the geometry of the cutting tool, etc. The output data, according to the proposed application, are: spindle speed (which can also be determined analytically from the input data), the feed (similarly, can be determined from the input data) and the vibration amplitudes related to the process in a discretized form. The discretization on frequency bands can be done depending on the performance of the network. Each band used for monitoring will essentially add another dimension to the tensor. It can be concluded that using a large number of frequency bands can lead to high network performance. In reality, the number of bands used must be optimized because it exponentially influences the training time and the minimum required number of samples.

### 4.3.1 Simulation of cutting process, cutting forces

As shown in Chapter 2.2.1.1.1.1, the literature provides a variety of analytical models that can be used in the estimation of cutting forces, but they introduce many simplifying assumptions. An alternative is to use finite element simulations, discussed more fully in Chapter 2.2.1.1.3, but these methods introduce a new problem related to computational costs. A possible solution is to reduce the number of finite elements by switching from an oblique (3D) to an orthogonal (2D) simulation model.

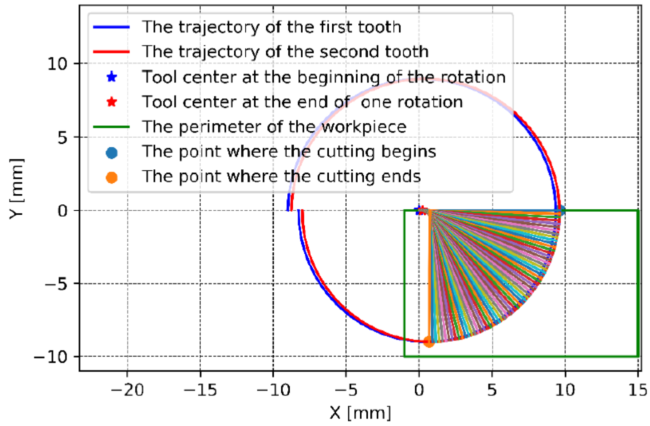


*Fig.. 4.10 The cycloidal trajectories of two consecutive teeth, workpiece perimeter with the start/end points and the instantaneous section generation* **[37]**

An original approach that further simplifies the finite element analysis for milling operations is presented in **[37]**, by changing the type of generating motion from rotation to rectilinear, the improved method being independent of the number of teeth of the cutting tool. In essence, the method proposes: extracting the chip section generated by the passage of one cutting tool tooth; running the orthogonal simulation using the unwrapped chip; recomposing the overall cutting force behavior using the cutting tool geometry information; wrapping the results back from the polar coordinate system to the more suited MU cartesian coordinate system based on the kinematics of the cutting process and finally extracting the final forces that can be applied on the MU model as loads to get the structural response.

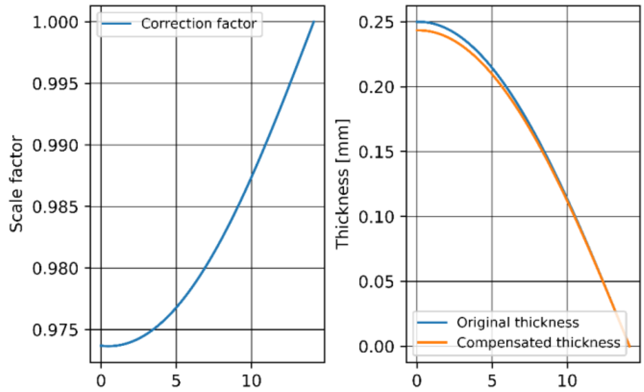


*Fig. 4.12 Curve correction factor (left), the original and the compensated thickness (right)* **[37]**

Due to the unfolding process (Fig. 4.10), the thickness variation must be adjusted by means of a correction factor calculated using the linear velocities (relation 4.1).

$$S_c(\emptyset) = \frac{Sc_1}{Sc_2} \qquad 4.1$$

where: $Sc_1$ [m/s]→ instantaneous speed of two consecutive points on the trajectory, 1st tooth;

$Sc_2$ [m/s]→ instantaneous speed of two consecutive points on the trajectory, 2nd tooth;

∅ [°]→ the rotation angle of the cutting tool.

The correction factor and the corrected thickness variation are shown in Fig. 4.12.

The computational cost of a simulation using this method was 1.5 days. Compared to the equivalent oblique simulation of 13.5 days, a decrease of ~89 % of the calculation time resulted.

### 4.3.2 Generating dynamic cutting samples using design space exploration techniques

Starting from the sample structure, it can be deduced that the theoretical maximum number of unique samples that can be obtained is directly influenced by the total number of input variables and the variation domain of each variable (the desired and/or imposed resolution being the discretizing factor). We can call this set of input data the "design space" of the system under study. In the context of the present research, this space is defined by the main characteristics of the cutting regime that directly influences the dynamic behavior of chip formation. Generating a representative set of training samples is directly influenced by how this design space is explored in order to expose meta-dependencies with the intention of later inoculating them into control AI algorithms. How this exploration takes place directly influences both the total cost of generating the sample set and the final performance of the AI control algorithm.

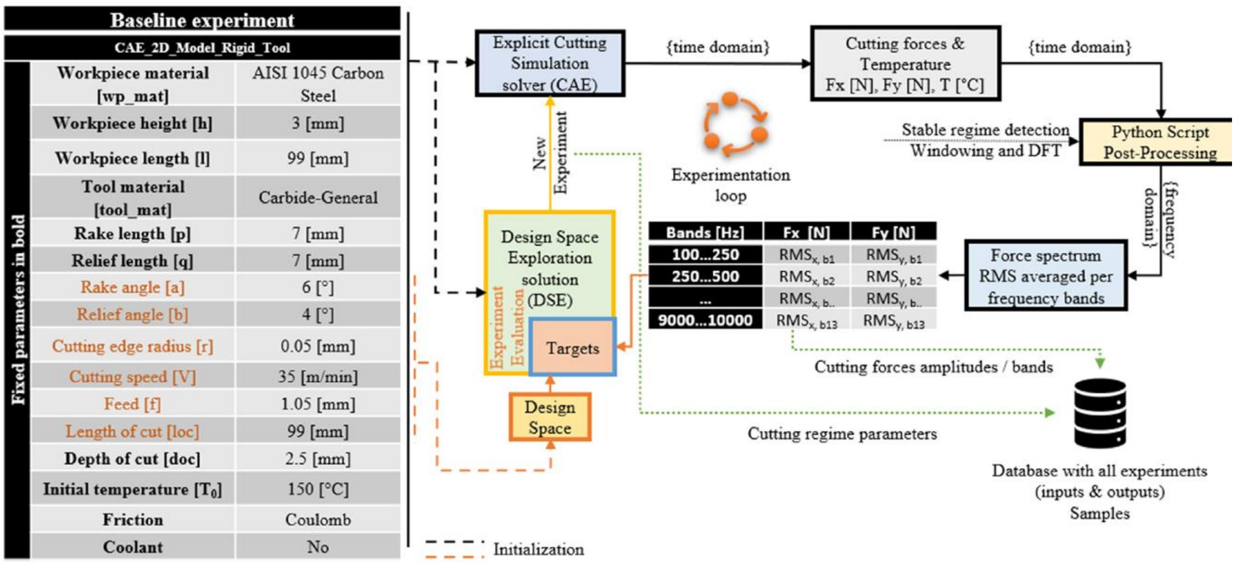


*Fig. 4.21 DSE loop for synthetic cutting data generation* **[41]**

An alternative to random explorations are the Design Space Exploration techniques (DSE), capable of traversing these spaces in a semi-automatic, online fashion. These analyses evaluate the results obtained and constantly optimize subsequent configurations.

A unique approach involving this kind of exploration, combined with cutting process simulation methods, was proposed in the work **[41]**. Similar to the paper **[37]**, the applicability, scalability and validity of the method were exposed by means of an example, the longitudinal turning of AISI1045 steel.

Fig. 4.21 shows the detailed diagram of the optimization loop used to generate samples related to the case in question. As can be seen, the design space for this case is defined by the left side of the scheme, containing parameters marked in orange ($a, b, r, V, f$ $și$ $loc$). The rest of the parameters are used for the construction of the orthogonal simulation model, they remain constant. The limitation of the design space was done as follows: $a = -8 \dots +8[°]$; $b = 0 \dots 8[°]$; $r = 0.02 \dots 0.1[mm]$; $V = 1 \dots 120 \left[\frac{m}{min}\right]$; $f = 0.1 \dots 2[mm]$.

The objectives set for this case are specific to the type of sample that is desired to be generated: maximizing the material removal rate by means of the $V$ $and$ $f$ parameters with the minimization of the vibration amplitudes on all frequency bands.

An empirical approach was used to validate the obtained data: the interpretation of the obtained data by means of the correlation factors calculated between various parameters, part of the design space, and the amplitudes obtained on the frequency bands (Fig. 4.24). Some clear mechanical trends are to be observed, such as the fact that the cutting speed $V$ influences both cutting forces $Fx$,$Fy$ similarly, something to be expected. A sign change is observed between band 6 and 7. This change validates another hypothesis applied in the industry, which relates the increase in cutting speed to the improvement of dynamic stability. Another anticipated trend can be observed, related to the influence of the feed $f$; it acts predominantly in the direction of the force $Fx$. Furthermore, it can be seen that this assumption does not apply when analyzing band 3, the effect suggesting the occurrence of a harmonic phenomenon.

| Cutting parameters: | V | | f | | a | | b | | r | | |
|---|---|---|---|---|---|---|---|---|---|---|---|
| Directions: | Fx | Fy | Fx | Fy | Fx | Fy | Fx | Fy | Fx | Fy | |
| **Band 1** (0.1…0.25 kHz) | 0.350 | 0.380 | 0.230 | 0.150 | -0.570 | -0.580 | -0.400 | -0.450 | -0.360 | -0.340 | Low frequencies |
| **Band 2** (0.25…0.5 kHz) | 0.160 | 0.240 | 0.480 | 0.370 | -0.590 | -0.630 | -0.540 | -0.500 | -0.370 | -0.330 | |
| **Band 3** (0.5…0.75 kHz) | 0.200 | 0.250 | 0.750 | 0.660 | -0.440 | -0.470 | 0.000 | 0.090 | -0.310 | -0.310 | |
| **Band 4** (0.75…1 kHz) | 0.160 | 0.250 | 0.540 | 0.230 | -0.550 | -0.630 | -0.580 | -0.570 | -0.330 | -0.310 | |
| **Band 5** (1…2 kHz) | 0.260 | 0.280 | 0.480 | 0.280 | -0.540 | -0.590 | -0.580 | -0.620 | -0.300 | -0.260 | Middle frequencies |
| **Band 6** (2…3 kHz) | 0.020 | 0.050 | 0.640 | 0.200 | -0.530 | -0.810 | -0.570 | -0.560 | -0.310 | -0.030 | |
| **Band 7** (3…4 kHz) | -0.110 | -0.140 | 0.610 | 0.030 | -0.600 | -0.860 | -0.550 | -0.230 | -0.310 | 0.240 | |
| **Band 8** (4…5 kHz) | -0.260 | -0.430 | 0.460 | 0.120 | -0.600 | -0.430 | -0.580 | -0.390 | -0.180 | 0.140 | |
| **Band 9** (5…6 kHz) | -0.410 | -0.520 | 0.360 | 0.060 | -0.640 | -0.250 | -0.440 | -0.270 | -0.120 | 0.150 | High frequencies |
| **Band 10** (6…7 kHz) | -0.590 | -0.610 | 0.080 | -0.030 | -0.460 | -0.120 | -0.270 | -0.160 | 0.150 | 0.180 | |
| **Band 11** (7…8 kHz) | -0.610 | -0.490 | -0.240 | -0.380 | -0.410 | -0.180 | -0.060 | 0.280 | 0.330 | 0.470 | |
| **Band 12** (8…9 kHz) | -0.460 | -0.430 | -0.360 | -0.370 | -0.330 | -0.250 | 0.160 | 0.260 | 0.440 | 0.540 | |
| **Band 13** (9…10 kHz) | -0.440 | -0.440 | -0.370 | -0.420 | -0.290 | -0.210 | -0.040 | 0.120 | 0.290 | 0.450 | |

| Correlation between the main cutting parameters | | f | a | b | r |
|---|---|---|---|---|---|
| | V | -0.02 | -0.07 | -0.1 | 0.04 |
| | f | | -0.13 | -0.13 | -0.22 |
| | a | | | 0.33 | -0.14 |
| | b | | | | 0.04 |

| | | |
|---|---|---|
| V | [m/min] | Cutting speed |
| f | [mm] | Feed |
| a | [°] | Rake angle |
| b | [°] | Relief angle |
| r | [mm] | Cutting edge radius |

| Legend | | |
|---|---|---|
| | 1.000 | Directly Proportional Correlation |
| | 0.000 | UNcorrelated |
| | -1.000 | Inversely Proportional Correlatio |

*Fig. 4.24 Correlation plot between the DSE inputs/outputs [41]*

Another very important parameter to investigate is the rake angle $a$. As can be seen, it has an inversely proportional correlation with both cutting forces, something anticipated, but the data suggests that it acts predominantly at low and medium frequencies. The same trend can be observed for the clearance angle $b$.

The last parameter investigated individually is the nose radius $r$. As already mentioned, this parameter is associated with the cutting tool wear level. Analyzing the obtained data, this influence can be observed at high frequencies, but not so obviously at low frequencies.

## 4.4 Determining the dynamic transfer functions of machine – tools

For the correct/complete description of the dynamic phenomenon in machining, it is not enough only to model the chip formation process. Next, the attention will be directed to the development of solutions that will allow the coupling of the simulated cutting forces with the dynamic characteristics of the machine tools. This coupling basically represents the determination of the stiffness $k_*$ and damping $c_*$ coefficients as functions of the cutting system parameters, applicable to the longitudinal turning operation.

The experimental setup consists of a CNC lathe PO PY GIM PLG-42 on which a cutting tool with removable inserts is mounted, SVJBL 2020K 16 produced by the company SANDVIK. The modeling, analysis and measurements were carried out with the help of the suite of hardware and software solutions developed by Siemens (NX, Simcenter, Simcenter HEEDS MDO, Simcenter Testlab and Simcenter SCADAS XS).

### 4.4.2 Modal evaluation of the cutting system for step turning operations with SVJBL 2020K 16 cutting tool

In order to be able to perform an assessment of the modal behavior of the longitudinal turning operation with the SVJBL 2020K 16 cutting tool, this research chapter focused on coupling the two main components that form the generator system, cutting tool and workpiece (Fig. 4.39).

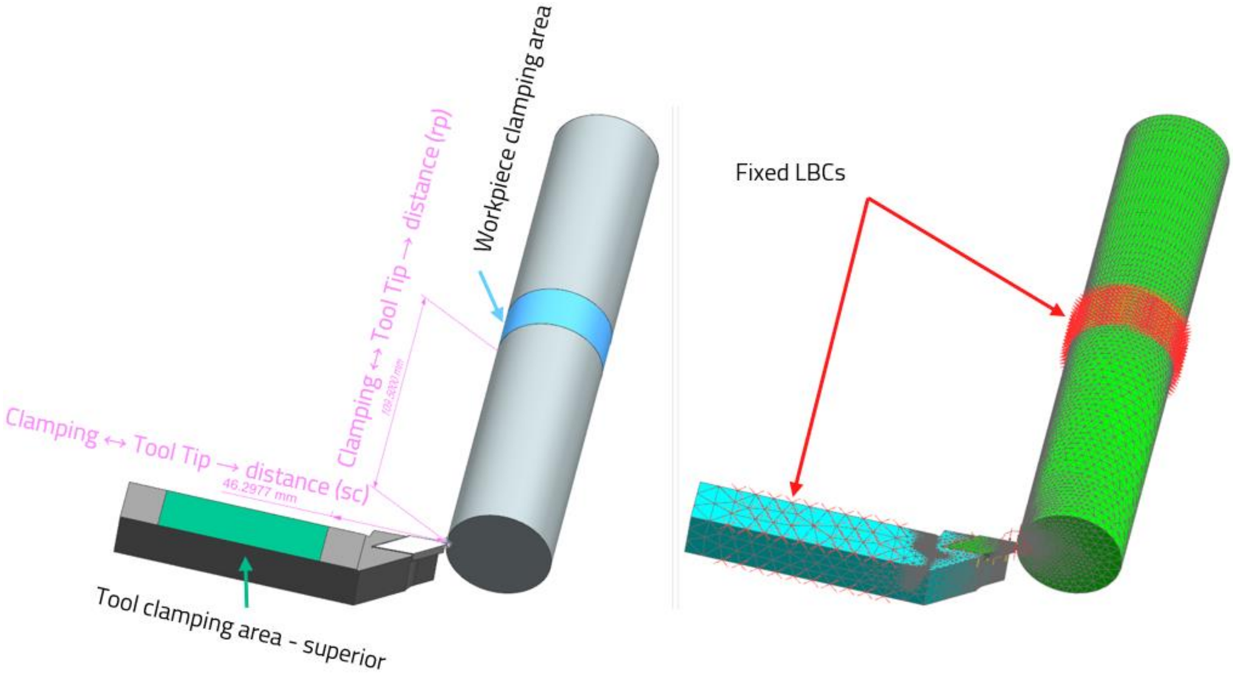


*Fig. 4.39 Cutting tool – workpiece assembly – CAD model (left) – FEM model (right)*

The analyses carried out had the same goal: exposing the critical characteristics and important parameters that influence the way the dynamics of the generator system can interact with the self-excitation vibration phenomenon.

Geometrically, the workpiece is a solid bar with a diameter of 42 [mm] and a total length of 230 [mm], both dimensions being constructively limited by the selected CNC lathe used in the experiments.

The material properties used are identical to those used for the cutting tool. In addition to the parameters already studied, the variation of the cutting forces and the distance variation between the tool clamping area and the tool-tip (sc), in this study a new dimensional variation was introduced representing the distance between the tool-tip and the workpiece clamping (rp) (Fig. 4.39). The diameter is constant, but the rp parameter of the workpiace can vary in the 0 ... 210 [mm] domain, limited by the length of the clamping system (20 [mm]) and the working space of the MU.

The workpiece clamping was modeled in the finite element analysis as for the cutting tool, with the cylindrical area describing the clamping being fully constrained. A peculiarity in this modeling is the way in which the quasi-static cutting forces were applied to the model. In practice, the dynamics of the chip formation process generate cutting forces that load both components identically, with opposite sign. Since in this analysis the chip formation process is not simulated (more details in Chapter 2.2.1.1.3), the forces are introduced using an original method, which reduces the interaction area to one-dimensional (1D) elements of type RBE2 and CBAR , on which a dedicated boundary condition is applied to model the forces usally used for bolts.

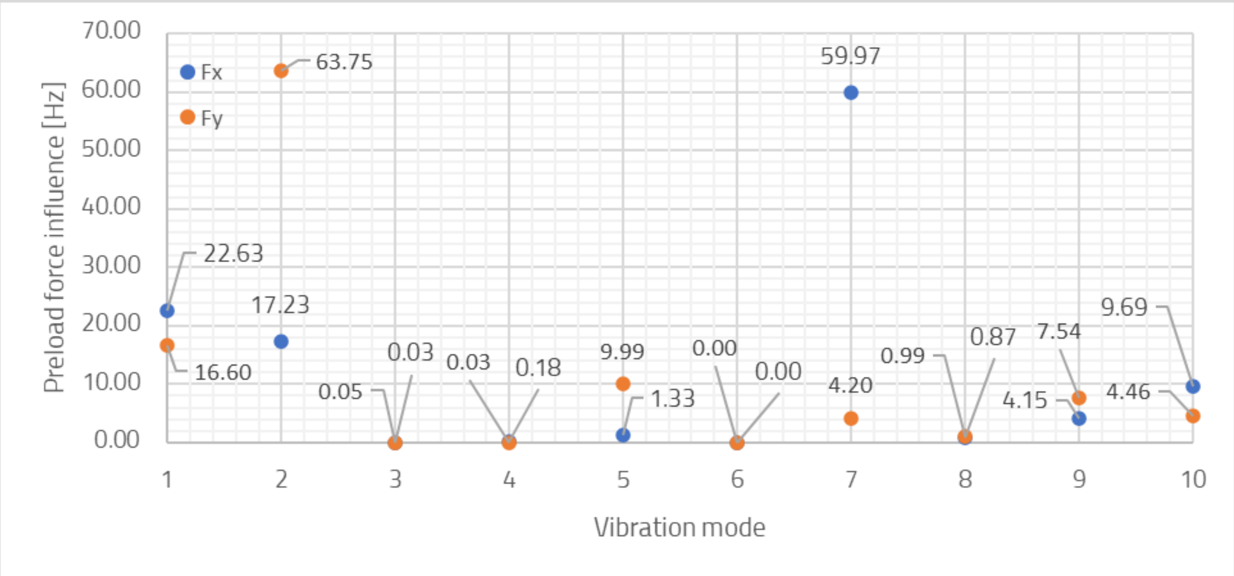


*Fig.. 4.41 The maximum influence of the cutting forces variation on the normal modes of the generator system*

Analyzing the obtained results (Fig. 4.41), it can be noted that each loading direction induces a significant change in the frequency of a different natural mode of vibration. The variation of the cutting force on the $Fx$ direction substantially modifies a natural mode of vibration that manifests itself through deformation predominantly in the $Fy$ direction, this mode being strongly correlated with the 1st mode of vibration obtained in the isolated modal analysis done on the cutting tool.

Regarding the variation of the cutting force in the $Fy$ direction, an equally significant influence can be observed on vibration mode 2, the bending mode in the Z direction. Analyzing the deformation shape for this case, it is observed that this mode is induced by the workpiece, without significant contribution from the cutting tool.

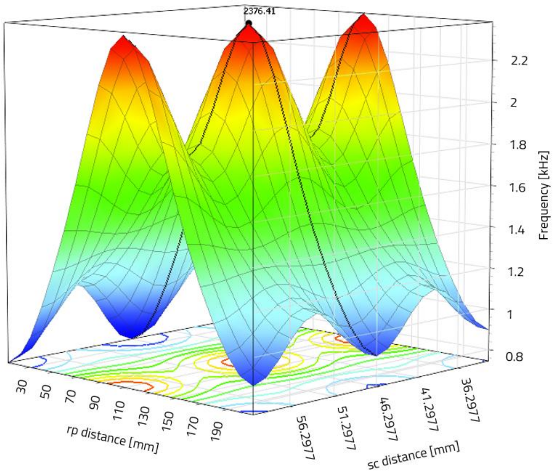


*Fig. 4.46 Sensitivity analysis – Kriging response surface for vibration mode 1*

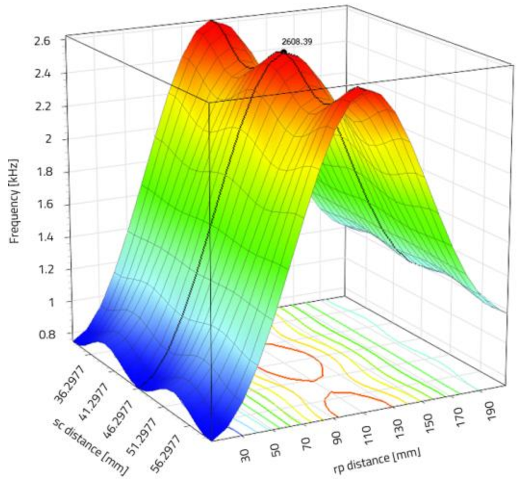


*Fig. 4.47 Sensitivity analysis – Kriging response surface for vibration mode 2*

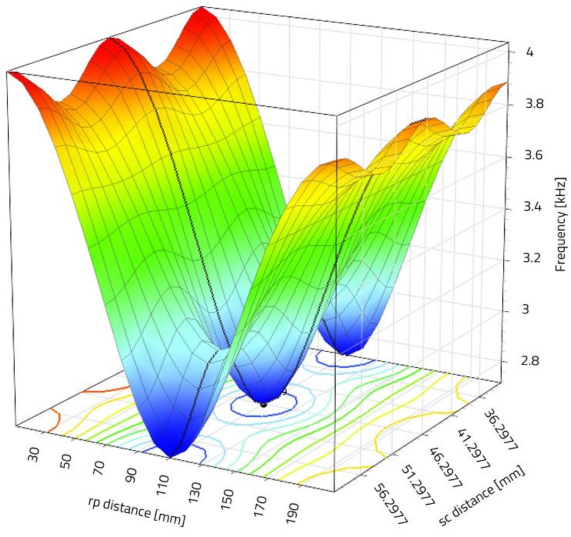


*Fig. 4.48 Sensitivity analysis – Kriging response surface for vibration mode 3*

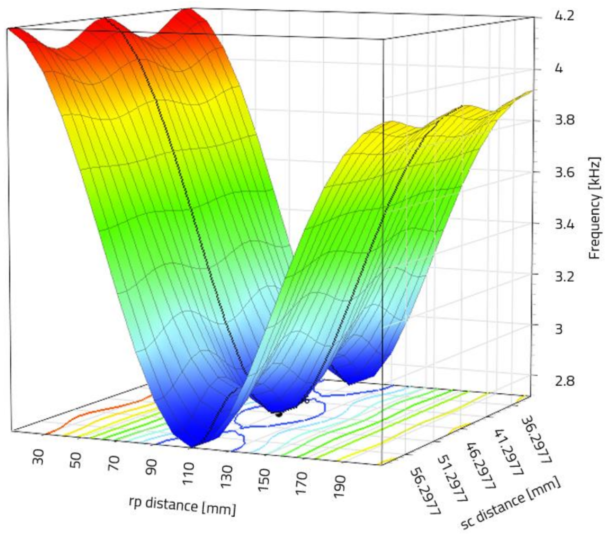


*Fig. 4.49 Sensitivity analysis – Kriging response surface for vibration mode 4*

In addition to the variation of 7th mode, the influence of the preload on the $Fx$ direction is also significant for modes 1, 2 and 10 (Fig. 4.41), the first two being bending modes that manifest predominantly on the workpiece, and mode 10 being a complex mode that indicates the appearance modal coupling between the two systems.

Similarly, the influence of the preload on the $Fy$ direction is visible not only on mode 2. Natural vibration modes 1, 7 and 10 (Fig. 4.41) also show significant changes in terms of the frequency at which they manifest. Modes 1 and 7 are bending modes in the $Fx$ direction, but mode 5 differs in its shape, being a torsional mode of the workpiece.

A comparative analysis of the results obtained up to this point suggests the elimination of preload forces (generated by cutting forces) from the list of the most important parameters that can intervene/modify the modal behavior in the longitudinal turning process. The influences are visible, as shown in the individual analyses, but compared to those generated by the variation of two distances they are several orders of magnitude smaller. For a better visualization of the complexity of the influences of the two remaining parameters, a series of sensitivity analyses were deployed. These graphs are generated using a factorial Kriging interpolation, interpolations able to handle with sufficient precision the complexity of the calculated response space [102]. Analyzing the results obtained for the first mode of vibration (Fig. 4.46), it can be observed that the distance between the tool-tip and the workpiace clamping (sc) is predominant, but the influence of the other distance (rp) is notable. For the 2nd vibration mode (Fig. 4.47) the sc paramater is less importat, but an asymmetry in the influence of the rp parameter also results. Modes 3 and 4 (Fig. 4.48 and Fig. 4.49) show a similar asymmetry in terms of the influence of the rp but, at the same time, an inversion of the distribution with resonance peaks positioned bordering on the variation domains.

### 4.4.3 Designing/prototyping the transfer functions measurement device for step turning operations on CNC PO PY GIM PLG-42 lathe

From an operational point of view, the modal behavior of the generating system can only be fully calculated and/or measured when all structural components and connections are considered. Not all of these components make a significant contribution in the end, but removing them from the start is not recommended.

Based on what was discussed in Chapter 4.4.2, it can be deduced that the use of finite element analysis is conditional on the modeling of the entire CNC PO PY GIM PLG-42 lathe to obtain the effective transfer functions. In the context of this research, it was decided to use the experimental method to determine these characteristics, because this method is more precise.

For the realization of the prototype/s, finite element simulations were used again, these being used for the dimensioning, validation and optimization of the basic concepts. The main objective pursued in this part of the research was the creation of a device capable of modeling the state of tension induced by the logitudinal turning operation on the CNC PO PY GIM PLG-42 lathe, using the SVJBL 2020K 16 cutting tool. In addition to the geometric accuracy, it was also imposed the development of a solution that allows the variation of the three analyzed parameters (cutting forces and the two distances sc and rp).

It was decided to measure the transfer functions using different devices for the two directions. The device designed to measure the preload in the $Fx$ direction (Fig. 4.56) was made starting from the geometrical information of the cutting tool discussed in Chapter 4.4.1.

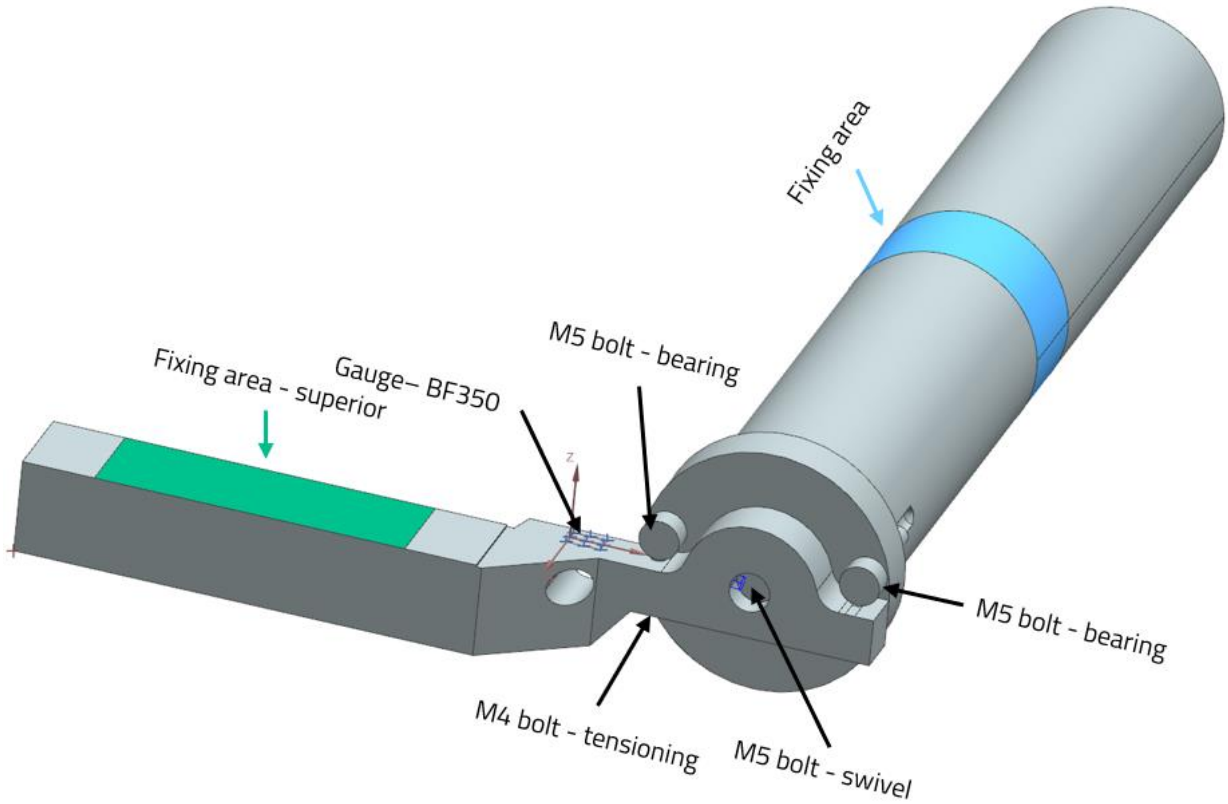


*Fig. 4.56 Transfer function measurement prototype in the Fx direction – CAD model*

A strain gauge (BF350) placed on top of the cutting tool is used to actually measure the applied force. The preload condition is achieved by means of a pivoting configuration around the axis of rotation of the workpiace.

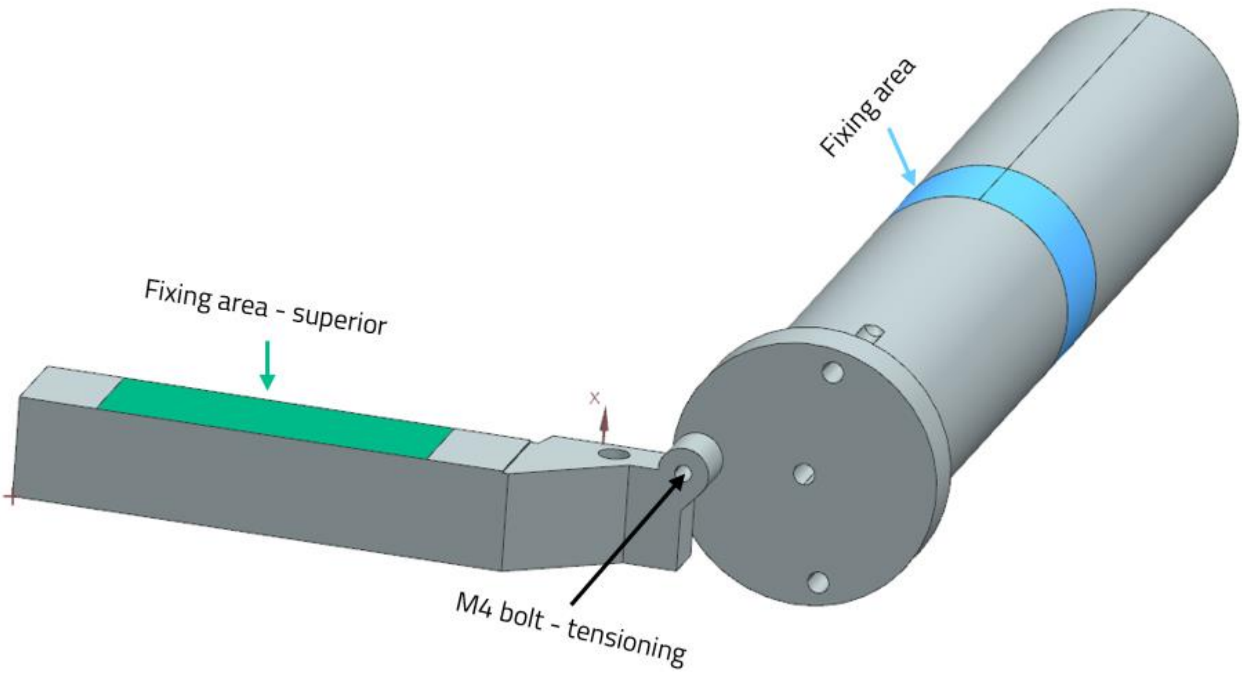


*Fig. 4.61 Transfer function measurement prototype in the Fy direction – CAD model*

To measure the preload forces in the $Fy$ direction, the same approach was used, with a simpler constructive solution, in the absence of the special conditions imposed by the free rotation of the spindle. The device assumes the most faithful modeling of the SVJBL 2020K 16 cutting tool, with the addition of an area that allows the use of an M4 screw that allows the application of a force between the two components (Fig. 4.61)

As can be seen, the workpiece model is reused for this configuration as well, it is not geometrically conditioned by any functional aspect.

##### *4.4.3.2 Instrumentation and calibration of the accelerance measurement devices with preload modeling*

As mentioned in the previous chapters, the measurement system developed for this research aims to measure the accelerance of the tool-tip point taking into account also the effect of the preload forces induced by the cutting process. In order to perform this type of measurement, it was decided to use the BF350 – 3AA strain gauges, functionally optimized in chapter 4.4.3.1, coupled with an acquisition system developed specifically for this application. System calibration was performed using configurations that allowed reproducing the clamping conditions on the tested machine tool (PO PY GIM PLG-42).

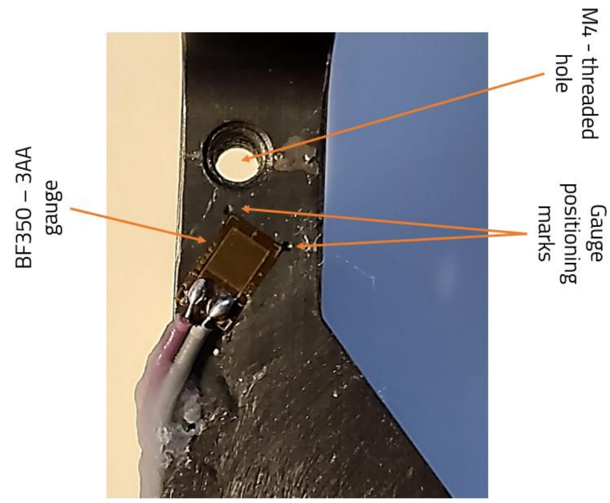


*Fig. 4.78 Transfer function device instrumentation with BF350-3AA strain gauge – Fx direction*

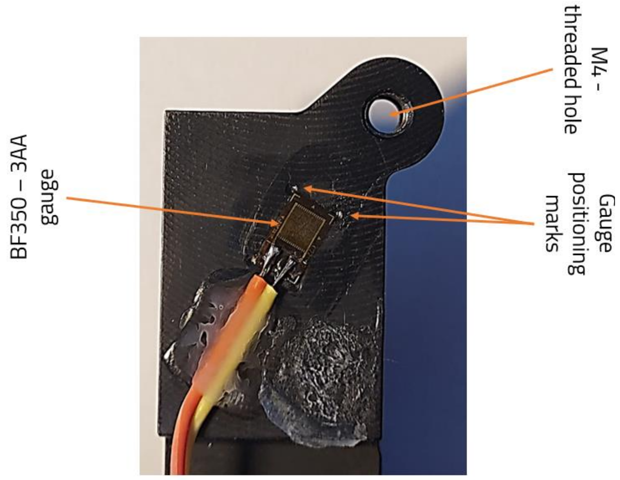


*Fig. 4.79 Transfer function device instrumentation with BF350-3AA strain gauge – Fy direction*

The instrumentation part involved the use of a Wheatstone bridge configuration, which in its complete form uses four active resistive elements. Due to geometric constraints, the use of the full bridge was not possible, the quarter-bridge configuration using only one active element being adopted.

The digital conversion is performed by means of a specialized ADC module (Fig. 4.81), HX711, capable of quantifying the electrical behavior of the Wheatstone bridge with a resolution of 24 [bit] (see Chapter 2.3.2.1).

The entire digital process is programmed and managed via an Arduino Uno development board connected directly to the HX711 module, which transmits the final data to the computer. The software component specially developed for this application is available in Appendix 3 –

Firmware for the preload force measuring devices used to measure the accelerance on CNC PO PY GIM PLG-42 (C++). Inducing the state of tension in the devices required the use of a configuration that allowed the orientation of the clamps according to the intended directions and the application of known masses for calibration. The calibration focused on only one position applied on the cutting tool, sc = 32.2977 [mm], the stiffest.

As can be seen in Fig. 4.80, the clamping of the measuring device in the $Fx$ direction was done by means of vises, obtaining the correct orientation with respect to the horizontal surface. The application of the loading force involved the use of the same type of M4 screw, connected to a loading table that self-aligns normal to the horizontal surface when left free. In the case of the measuring device in the $Fy$ direction (Fig. 4.81), the configuration is simpler, only one vise being used.

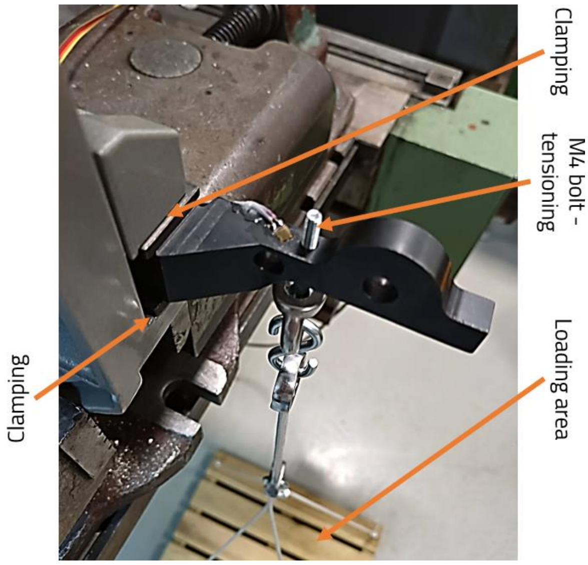


*Fig. 4.80 Calibration configuration of the measuring device - Fx direction*

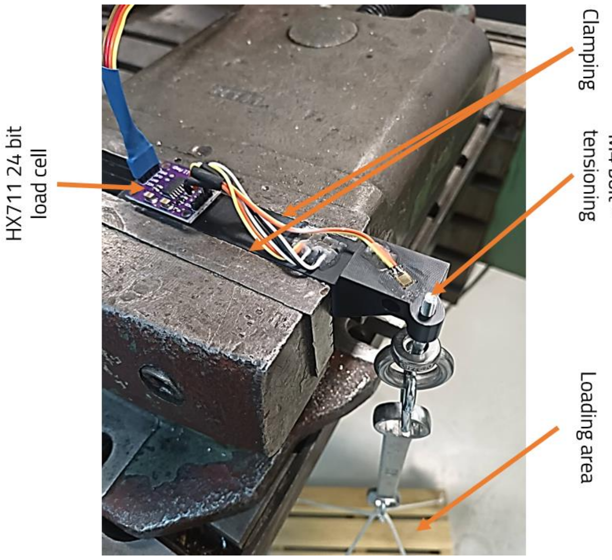


*Fig. 4.81 Calibration configuration of the measuring device - Fy direction*

The calibration procedure involved reading the digitized values in 22 load positions, starting from 0 [kgf] to values close to those corresponding to a load force of ~ 61 [kgf]. It was decided to calibrate the systems in the force range 0 ... 600 [N], the cutting force range valid for the studies to be carried out in this paper. The total load mass was validated for each position using an electronic balance placed on the same base surface of the system and which has a measurement accuracy of +/- 1 [g], the increment used being ~ 2.5 [kgf].

### *4.4.3.3 Performing experimental measurements*

Physical tests were performed on two configurations: one to measure the accelerance of the SVJBL 2020K 16 tool mounted on the tool holder system and the other to measure the accelerance of the tool-tip using the devices developed in the previous chapters.

Data measurement, acquisition and post processing were done using an accelerometer manufactured by PCB (333B30), connected to a Siemens SCADAS XS system and using the Siemens Test Lab software solution (Fig. 4.86). The measurement of accelerance involves the use of a modal hammer also produced by PCB (086C03) to generate the necessary energy reference.


*Fig. 4.86 Generic setup for measuring tool-tip inertances on the PO PY GIM PLG-42 CNC lathe*

In the first phase, the accelerance of the tool-tip point was mapped in the two directions, Fx and Fy, over the entire adjustment range of the machine tool X – Z. At the same time, 3 sc values were tested ( sc = 32.2977 [mm] (Fig. 4.88); 48.2977 [mm] and 61.2977 [mm] (Fig. 4.89)), a parameter that presented significant influences on the dynamic behavior according to the analyzes carried out in Chapter 4.4.2.

Instrumentation of the measured area involved removing the detachable components and mounting the accelerometer using a special glue. For the measurement in the $Fy$ direction, the accelerometer was mounted as close as possible to the tool-tip point, using the same special mounting glue (Fig. 4.90 and Fig. 4.91). The X – Z adjustment range was defined using as reference "0" the point of intersection between the spindle axis and the minimum X position allowed by the workpiece clamping system.

The actual measurements involved striking the tip point area using the modal hammer, in the direction of interest and repeating each measurement 5 times to ensure the accuracy of the results. The results measured in the position X = 0 [mm] and Y = 0 [mm] can, theoretically, be compared with the results calculated in Chapter 4.4.1, because this point represents the position of maximum stiffness of the machine tool. If these results are analyzed in both directions, Fig. 4.96 and Fig. 4.97, it can be seen that the dynamic stiffness trends are compatible, but offset. The gap-related aspect can be explained simply by the major difference in stiffness of the two configurations; the simulations induce a massive stiffening of the mechanical system, while the measurements introduce the real stiffnesses and dampings of the entire kinematic chain of the machine tool.

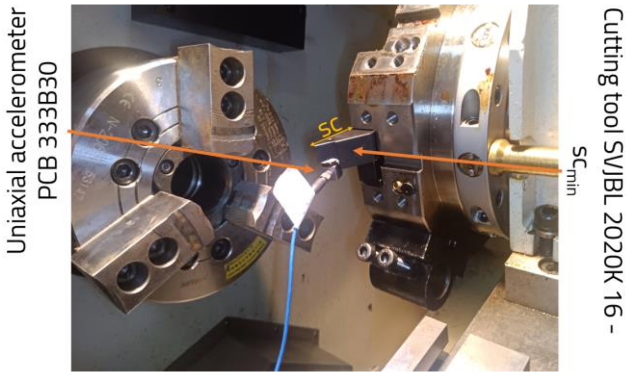


*Fig. 4.88 Inertance measurement in the Fx direction on the SVJBL 2020K 16 cutting tool without preload – sc = 32.2977 mm*

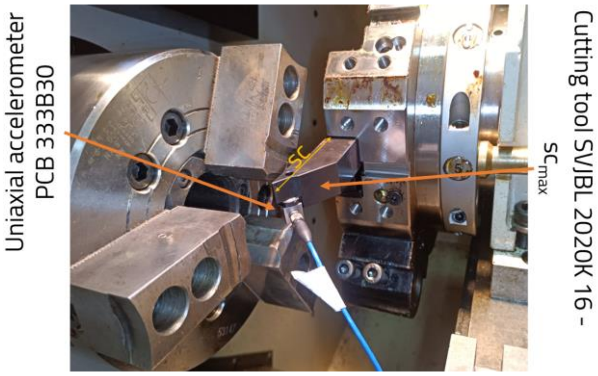


*Fig. 4.89 Inertance measurement in the Fx direction on the SVJBL 2020K 16 cutting tool without preload – sc = 61,2977 mm*

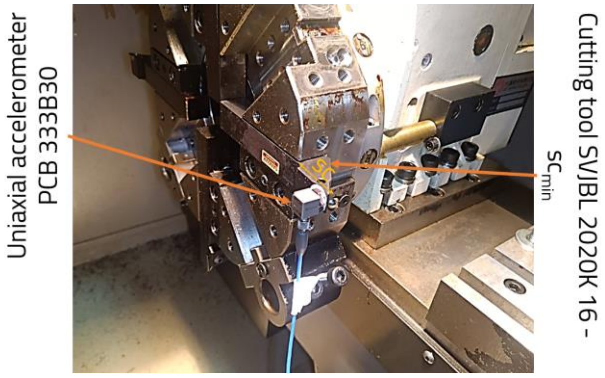


*Fig. 4.90 Inertance measurement in the Fy direction on the SVJBL 2020K 16 cutting tool without preload – sc = 32,2977 mm*

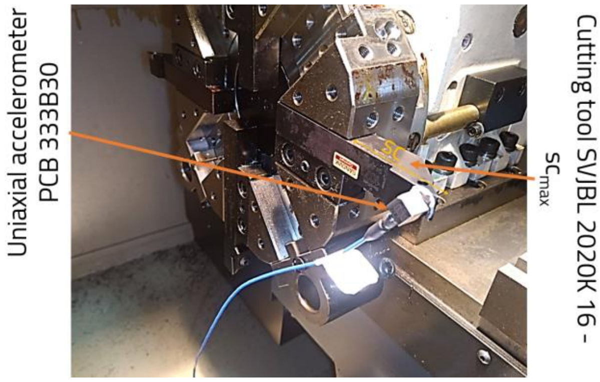


*Fig. 4.91 Inertance measurement in the Fy direction on the SVJBL 2020K 16 cutting tool without preload – sc = 61,2977 mm*

For both directions, flexibility peaks independent and dependent on the $sc$ parameter can be observed. Physically, the independent peaks can be associated with the dynamic behavior of the machine tool, and the dependent peaks with the isolated dynamic behavior of the cutting tool.

The results obtained in this part of the research confirmed the need to add the $X$ – $Z$ parameters as variables in the design space proposed in Chapter 4.3.2.

The measurement of the accelerance of the generator system with the preload modelling, using the specially designed devices, was performed following the same procedure. Different from the previous measurements is the fact that the workpiece is materialized in this case, an aspect that can influence the dynamics of the system through its simple mass.

Due to the fact that the devices were calibrated only for the assembly configuration $sc = 32.2977$ $[mm]$, the measurements carried out do not expose the possible influences that this parameter may have on inertia.

The system was designed to measure a single processing diameter of the semiconductor, $\Phi = 21$ $[mm]$, so the adjustment space $X - Z$ is defined in this case with $X$ constant.

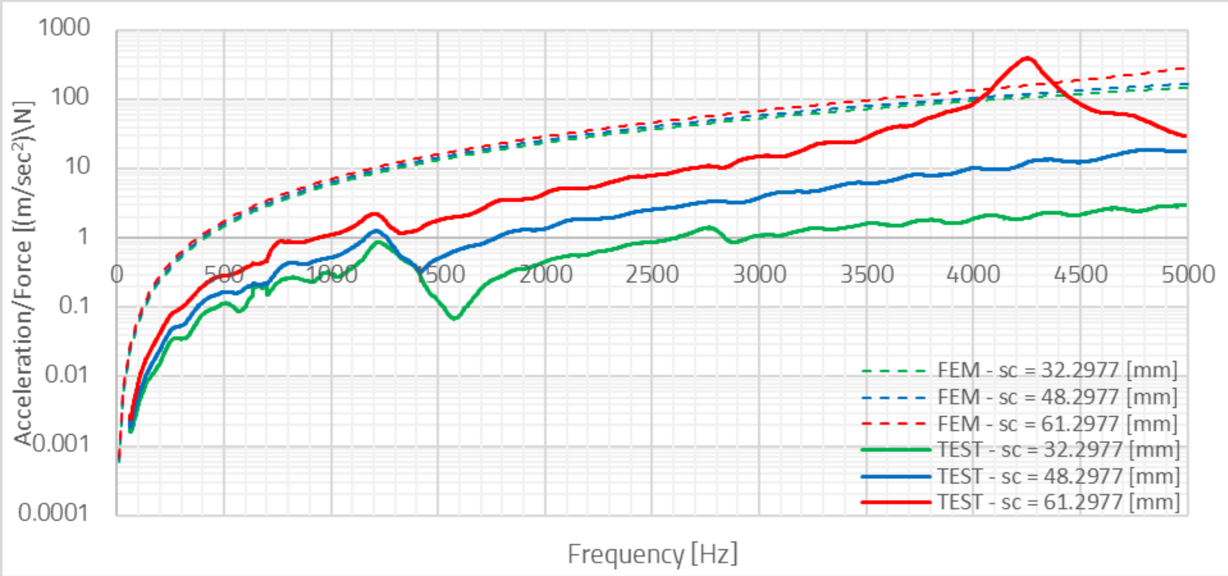


*Fig. 4.96 Inertances in the Fx direction for the minimum, average and maximum position (sc) of the SVJBL 2020K 16 cutting tool for the X = 0 mm; Z = 0 mm coordinates measured on the PO PY GIM PLG-42 CNC lathe and compared with the inertances calculated with FEM*

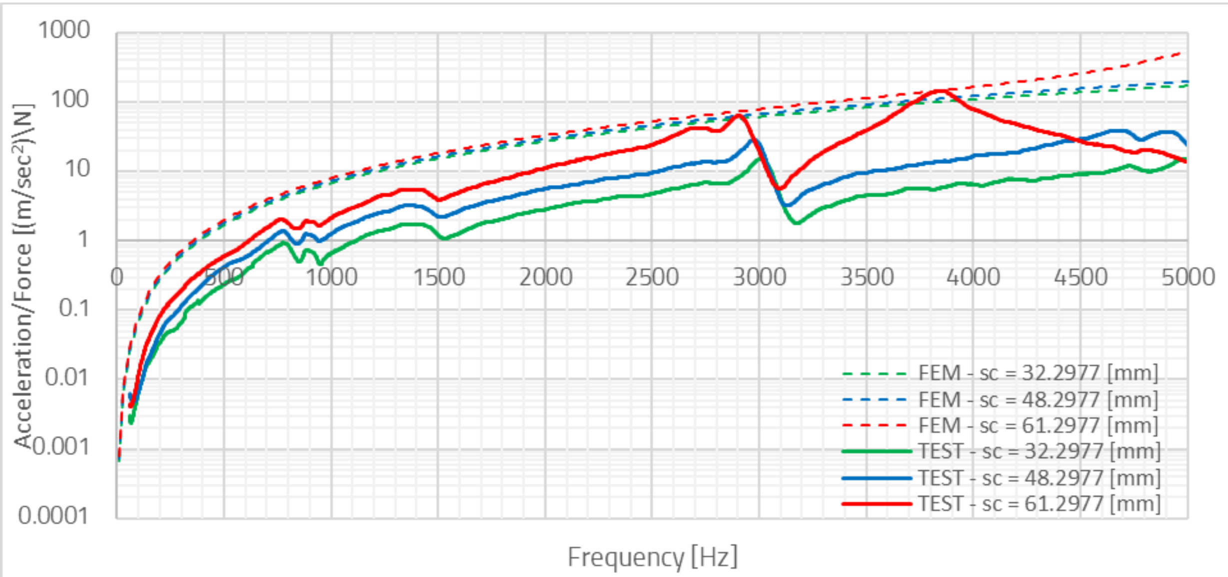


*Fig. 4.97 Inertances in the Fy direction for the minimum, average and maximum position (sc) of the SVJBL 2020K 16 cutting tool for the X = 0 mm; Z = 0 mm coordinates measured on the PO PY GIM PLG-42 CNC lathe and compared with the inertances calculated with FEM*

Measurements were carried out on 5 positions of this parameter, $Z = 30{,}60{,}90{,}120$ and $150$ $[mm]$, using the same reference.

As can be seen in Fig. 104 and Fig. 4.105, the pretensioning device was mounted in the tool - holder, the accelerometer being arranged as close as possible to the area of the theoretical generator point. Similarly, the configuration for measuring inertances in the $Fy$ direction (Fig. 4106 and Fig. 4.107) involved mounting the device in the revolver head and positioning the accelerometer in the correct direction of measurement.

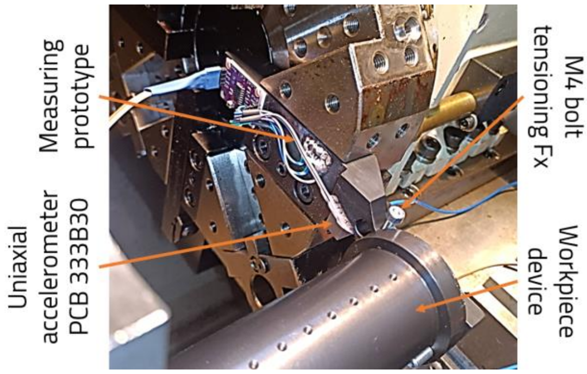


*Fig. 4.104 Fx inertance measuring device configuration with preload, $sc_{constant}$ = 32,2977 mm, $X_{constant}$ = 21 mm*

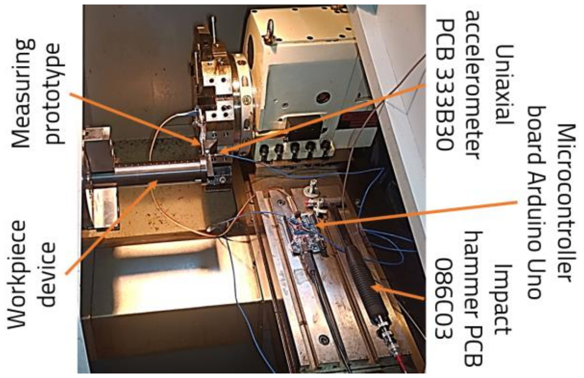


*Fig. 4.105 Fx inertance measuring device configuration with preload, $sc_{constant}$ = 32,2977 mm, $X_{constant}$ = 21 mm*

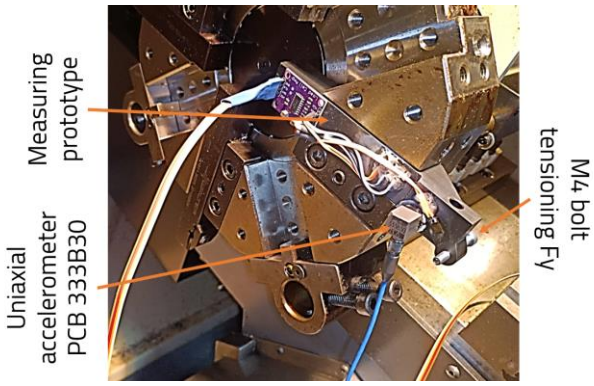


*Fig. 4.106 Fy inertance measuring device configuration with preload, $sc_{constant}$ = 32,2977 mm, $X_{constant}$ = 21 mm*

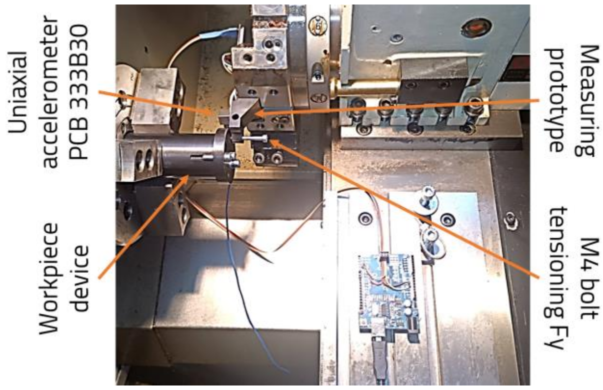


*Fig. 4.107 Fy inertance measuring device configuration with preload, $sc_{constant}$ = 32,2977 mm, $X_{constant}$ = 21 mm*

The adjustment of the preload force is carried out by means of the M4 screws, the preset value being confirmed by the computer and the acquisition system. It was decided to measure the inertances for each configuration from 0 to 600 [N] with a 100 [N] step.

The result for the first test configuration is shown in Fig. 4108 and Fig. 4.109 relating to inertances in the directions $Fx$ and $Fy$ respectively. Analysis of the results shows that the generator system shows significant variations in different pre-load states, but these are minimized by the dynamic characteristics of the entire system.

For clarity, and with the same simplifying assumptions regarding how the constraints applied in the FEM/MEF analyses can influence the dynamics of the structural response, it was decided to add the inertity curve for the generator system simulation with pre-load of 532.2 [N]. Similar to the isolated knife analysis, for both directions, dynamic trends are correlated. For the Fx case, two areas of interest can be observed, the decrease in rigidity around the frequency of ~1400 [Hz] and the correlation point of measurements with the simulated results from 3200 [Hz]. The decline in rigidity may have several explanations but in the context of this work this aspect is not relevant, important to understand is the phenomenon of 3200 [Hz]. For both directions, it can be noted that after reaching this critical frequency, compared to the calculated inertia, the gap is more pronounced.

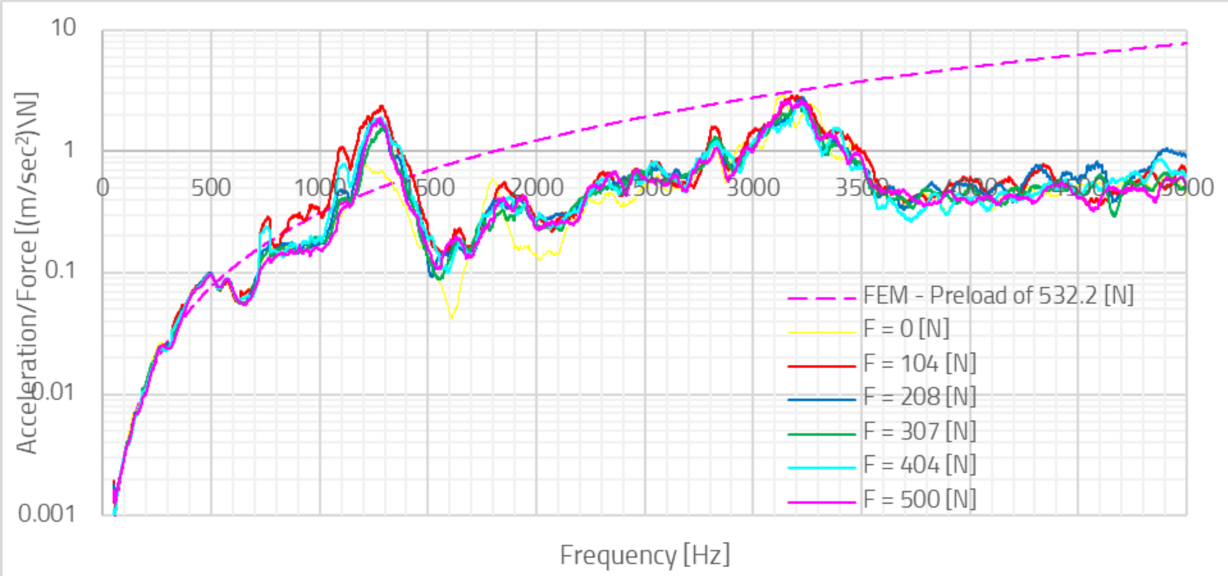


*Fig. 4.1 Inertances in the Fx direction measured on PO PY GIM PLG-42 CNC lathe with the pre-tensioning device for X = 21 mm Z = 30 mm coordinates, sc = 32.2977 mm compared with the closest FEM reference*

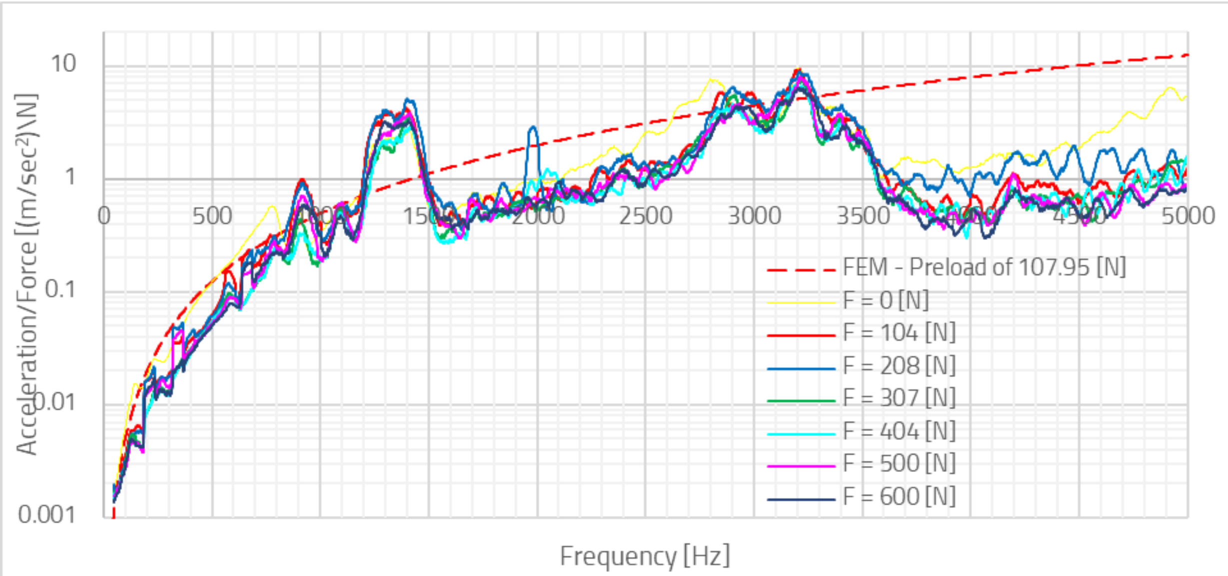


*Fig. 4.2 Inertances in the Fy direction measured on PO PY GIM PLG-42 CNC lathe with the pre-tensioning device for X = 21 mm Z = 30 mm coordinates, sc = 32.2977 mm compared with the closest FEM reference*

## 4.6 Training and testing of neural networks with synthetic samples

As presented in Chapter. 4.1 and Chapter.4.2, artificial intelligence uses a wide variety of solutions and methods to optimize training performance and prediction.

The structure of the neural network studied in this chapter can be described through Fig. 4.128. The input layer contains only two neurons representing the two parameters, $sc$ and $rp$. The output layer consists of 20 neurons, each representing the RMS value of the acceleration on a frequency band to be estimated by the network. This structure is the basis of any system solution for the detection and/or control of the phenomena studied by this paper, the complexity of the parametric space concerned being fundamental in its construction. The hidden layers can vary both in number and by the number of neurons defined on each layer. Choosing an optimal configuration for defining these hidden layers involves balancing prediction performance with computational costs.

In a real engineering application, an active control system of any dynamic phenomenon implies a rapid and accurate response of the system coupled with a high capacity of correct self-training, guided by configurations that generate new behaviors (samples).

This research is focused on a small component of the proposed sample concept, the analysis of the whole system may be the subject of future advanced studies. A complete variant of the imagined system would assume the existence of this agent capable of correctly discriminating online measured signals on monitored/controlled systems and, if necessary, to trigger both corrective actions to avoid the occurrence of the phenomenon of autovibration and self-training actions for actions without effect or those that worsen the dynamic state of the system. This summary description is based on the use of a reaction loop concept, where the validation and pre-training of the fundamental module for estimating the dynamic state of scaling processes is complementary.

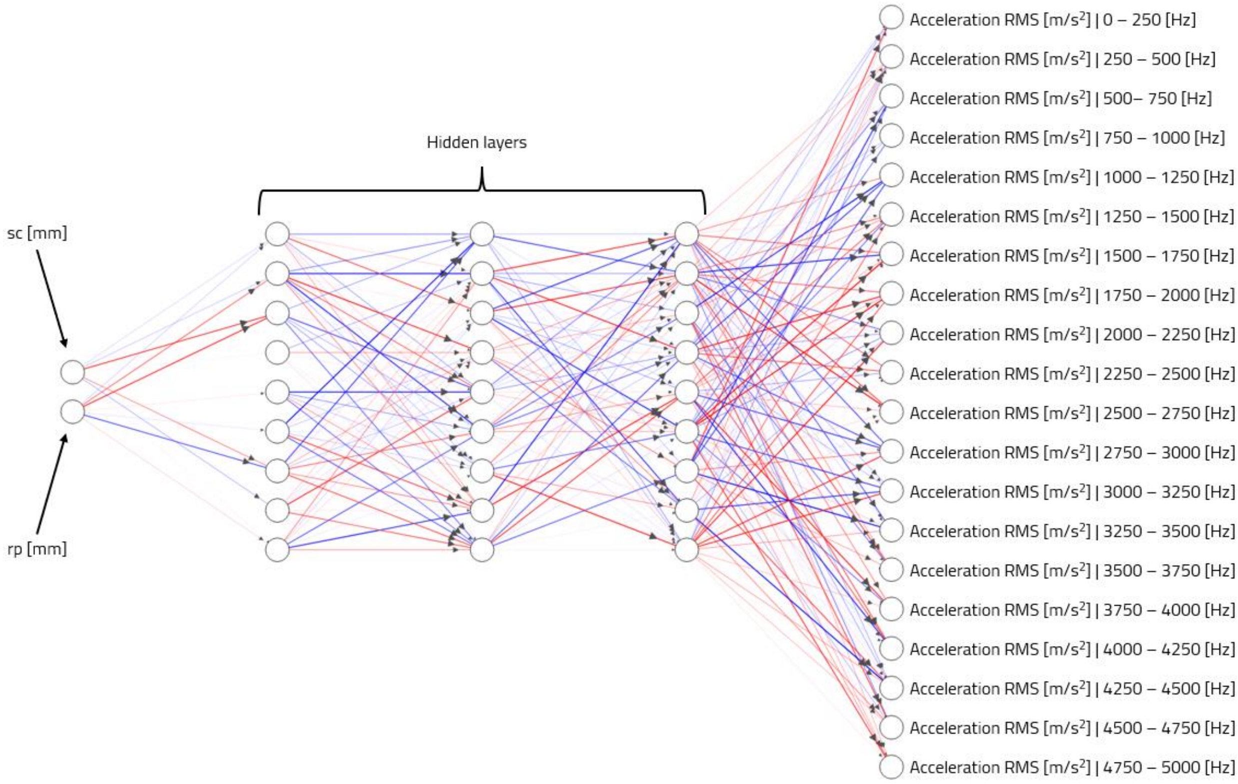


*Fig. 4.128 Neural network structure for estimation of tool point accelerations*

Based on the synthetic data obtained in Chapter. 4.5.1, calculable and hybrid data using actual transfer functions measured in Chapter. 4.4.3.3, it was possible to construct a collection of 6061 dynamic samples of the targeted cases in the MU's geometric adjustment space given by the parameters $sc$ and $rp$. Using this data set, several configurations of neural networks have been built and tested to expose their accuracy and critical aspects that can influence both precision and computational performance.

*Tabel 4.3 The main configurations tested in order to generate neural networks for predicting the accelerations of the generating system*

| Iteration | Neural network structure | | | | | Hyperparameters | | | Accuracy [%] | | | | | |
|---|---|---|---|---|---|---|---|---|---|---|---|---|---|---|
| | | | | | | | | | Activation | | | | | |
| | Input layer | Hidden layer 1 | Hidden layer 2 | Output layer | Parameters | Learn Rate | Epoch | Batch Size | ReLU | | LeakyReLU | | PReLU | |
| | | | | | | | | | Fx | Fy | Fx | Fy | Fx | Fy |
| 1 | 2 | 0 | 0 | 20 | 20 | 0.001 | 100 | 50 | 0.00 | 0.00 | 0.00 | 0.00 | 0.00 | 0.00 |
| 8 | 2 | 9 | 0 | 20 | 227 | 0.001 | 2000 | 50 | 77.38 | 97.41 | 82.76 | 97.75 | 83.46 | 96.97 |
| 9 | 2 | 9 | 0 | 20 | 227 | 0.0005 | 2000 | 50 | 81.51 | 95.74 | 78.64 | 97.67 | 83.55 | 97.48 |
| 11 | 2 | 9 | 0 | 20 | 227 | 0.0005 | 3000 | 75 | 75.71 | 97.17 | 80.61 | **97.94** | **86.91** | 97.18 |
| 13 | 2 | 9 | 0 | 20 | 227 | 0.00025 | 3000 | 100 | 78.29 | 97.57 | 79.86 | 97.48 | 79.60 | 97.64 |
| 16 | 2 | 4 | 5 | 20 | 157 | 0.0005 | 1000 | 50 | 76.94 | 95.78 | **76.95** | 97.61 | 75.10 | 95.52 |
| 18 | 2 | 4 | 5 | 20 | 157 | 0.0005 | 1000 | 100 | 70.75 | 97.63 | 66.12 | **97.65** | 76.52 | 97.32 |
| 19 | 2 | 4 | 5 | 20 | 157 | 0.00025 | 1000 | 100 | 72.81 | 97.39 | 73.61 | 97.32 | 67.42 | 97.52 |
| 22 | 2 | 15 | 0 | 20 | 365 | 0.001 | 1500 | 50 | 81.02 | 98.01 | 81.71 | 98.44 | 87.00 | 97.67 |
| 25 | 2 | 15 | 0 | 20 | 365 | 0.001 | 1500 | 75 | 80.38 | 97.14 | 84.05 | 97.75 | 87.41 | 97.85 |
| 26 | 2 | 15 | 0 | 20 | 365 | 0.001 | 2000 | 75 | 84.76 | 97.81 | 87.39 | 97.70 | **90.21** | 97.24 |
| 27 | 2 | 15 | 0 | 20 | 365 | 0.001 | 3000 | 75 | 86.82 | 97.23 | 84.02 | **98.55** | 88.96 | 97.38 |
| 28 | 2 | 7 | 8 | 20 | 265 | 0.001 | 100 | 50 | 75.29 | 95.75 | 78.17 | 97.80 | 77.12 | 96.41 |
| 29 | 2 | 7 | 8 | 20 | 265 | 0.001 | 500 | 50 | 75.77 | 97.65 | 76.38 | 97.50 | 85.39 | 96.71 |
| 30 | 2 | 7 | 8 | 20 | 265 | 0.001 | 1000 | 50 | 83.08 | 97.47 | 84.75 | 97.67 | 83.58 | 97.48 |
| 31 | 2 | 7 | 8 | 20 | 265 | 0.001 | 2000 | 50 | 78.43 | 97.51 | **85.74** | 97.42 | 81.79 | **98.13** |
| 35 | 2 | 7 | 8 | 20 | 265 | 0.001 | 2000 | 75 | 81.90 | 97.86 | 84.10 | 97.68 | 82.97 | 96.52 |
| 39 | 2 | 69 | 0 | 20 | 1607 | 0.0005 | 2000 | 50 | 89.54 | 98.76 | 87.50 | 98.24 | **90.43** | **99.07** |
| 42 | 2 | 69 | 0 | 20 | 1607 | 0.00025 | 4000 | 50 | 86.86 | 98.39 | 88.78 | 98.60 | 88.99 | 98.51 |
| 43 | 2 | 69 | 0 | 20 | 1607 | 0.0005 | 2000 | 75 | 89.87 | 98.46 | 89.41 | 98.32 | 88.14 | 97.64 |
| 44 | 2 | 69 | 0 | 20 | 1607 | 0.0005 | 3000 | 75 | 89.24 | 97.77 | 90.41 | 98.22 | 89.62 | 98.27 |
| 47 | 2 | 10 | 59 | 20 | 1879 | 0.0005 | 500 | 50 | 89.64 | 98.41 | 88.72 | 97.05 | 90.32 | 97.24 |
| 49 | 2 | 10 | 59 | 20 | 1879 | 0.00025 | 1000 | 50 | 90.36 | 98.14 | 86.78 | 97.12 | 89.26 | 98.43 |
| 50 | 2 | 10 | 59 | 20 | 1879 | 0.00025 | 2000 | 50 | 89.25 | 98.83 | 88.74 | 98.54 | 90.04 | 97.92 |
| 52 | 2 | 10 | 59 | 20 | 1879 | 0.00025 | 4000 | 50 | 87.92 | 98.45 | **90.43** | **99.00** | 85.51 | 97.93 |
| 59 | 2 | 20 | 49 | 20 | 2089 | 0.0005 | 2000 | 50 | 87.83 | 98.04 | 89.46 | 98.98 | 83.49 | 98.87 |
| 60 | 2 | 20 | 49 | 20 | 2089 | 0.0005 | 3000 | 50 | 88.92 | 97.87 | 86.66 | 98.66 | **90.32** | **99.14** |
| 61 | 2 | 20 | 49 | 20 | 2089 | 0.0005 | 4000 | 50 | 89.58 | 98.53 | 89.84 | 98.60 | 88.05 | 98.84 |
| 64 | 2 | 30 | 39 | 20 | 2099 | 0.001 | 1000 | 50 | 90.43 | 97.99 | 88.10 | **98.87** | 88.28 | 98.85 |
| 66 | 2 | 30 | 39 | 20 | 2099 | 0.0005 | 1000 | 50 | 88.88 | 98.79 | 90.02 | 97.59 | 88.27 | 98.45 |
| 68 | 2 | 30 | 39 | 20 | 2099 | 0.00025 | 2000 | 50 | 89.36 | 98.11 | 88.98 | 96.89 | **90.85** | 98.03 |
| 71 | 2 | 40 | 29 | 20 | 1909 | 0.001 | 500 | 50 | 88.23 | 98.12 | 84.71 | 96.65 | 88.06 | 98.66 |
| 72 | 2 | 40 | 29 | 20 | 1909 | 0.001 | 1000 | 50 | 89.71 | 98.77 | 87.38 | 98.51 | 88.32 | 97.70 |
| 74 | 2 | 40 | 29 | 20 | 1909 | 0.0005 | 2000 | 50 | 89.20 | 98.37 | 89.73 | **98.80** | 86.05 | 98.28 |
| 76 | 2 | 40 | 29 | 20 | 1909 | 0.0005 | 2000 | 100 | 87.98 | 97.89 | **89.90** | 98.55 | 89.12 | 97.49 |

Based on the information of convergence, loss evolution and computational performance, configurations that influence beneficial training behaviors were selected and tested, eventually obtaining Table 4.3. This table (plus Annex 5) essentially shows the evolution of this process of manual exploration of the configuration and adjustment possibilities of neural networks used in estimating dynamic load spectrum in cutting processes for data sets of varying complexity.

To facilitate the identification of the constructive variants tested, in this study it was decided to use suggestive names, for example N2_N69_N20, representing a neural network with visible layers with 2 neurons on the input and 20 on the output, to which an invisible layer with 69 neurons was added.

The main configurations tested and the results obtained are presented in Table 4.3. The full version with all the tests performed can be found in Appendix 5 – Summary of all configurations tested on neural networks. Construction, hyperparameters, activations and reported accuracy.

Hyperparameter optimization was done manually with the aim of achieving a prediction accuracy of 90% with a minimum computational cost.

For the critical analysis of the computational performance of the 3 activation functions used in the training of neural networks, it was decided to use a normalized metric, the product between the number of training parameters and number of epochs used.

It can be noted that for the $Fx$ direction, PReLU activation is the most effective, followed by ReLu activation. For the $Fy$ direction, the same activation function is confirmed as the most effective, followed by the LeakyReLU activation. A significant difference appears, however, in this case; the PReLU activation shows an evolution that suggests the possibility of further improving the accuracy achieved by increasing the number of epochs.

## 4.7 Conclusions

The fourth industrial revolution (Industry 4.0) has aggressively introduced and promoted the use of digital technologies in order to increase the level of autonomy in machining centers. There was already a solid digital foundation implemented through computerized numerical control interfaces (CNC → Industry 3.0), but it did not have the ability to provide monitoring/control of complex dynamic phenomena such as chatter. Artificial intelligence is currently at the forefront of this revolution, with its presence in industrial (and not only) fields growing exponentially.

Numerous teams of researchers are working intensively to implement and test these technologies for the detection and control of dynamic phenomena, reporting promising results in terms of accuracy.

The implementation of these techniques involves the use of several mathematical devices such as STFT, WT, WPD, HHT, EMD, VMD or LMD, all used in the pre-processing of measured physical signals in order to make them compatible with the intelligent control system.

The main obstacle to implementing AI technologies is the size of the data set needed for training. In the context of chatter control in MUs, this problem becomes even more evident due to the high costs involved with physical testing.

An alternative to physical testing is the use of finite-element simulations. Although the computing technology has evolved a lot in recent years, generating a suitable set of training data involves high computational costs that question the applicability of these methods in the AI training process. There is, however, a method to improve these computational performances by converting oblique scaling problems into orthogonal problems that can increase efficiency by ~90%.

In order to properly reconstruct the dynamics induced by a more complex cutting process like milling, an innovative method of deployment/wrapping of the cutting result can be extended to any type of processing.

Another critical aspect when it comes to generating the training set is related to defining and exploring the parametric space of interest. This step can be done randomly or using special exploration algorithms that can expose system interdependence much more efficiently. This research used a commercial solution, Siemens HEEDS MDO, in synergy with cutting simulations that allowed 25 cases to be generated in a short time with modest computational resources, validating the scalability of the method.

Evaluation of the modal component of the entire generator system can be done through finite-element simulations, but modeling difficulties often arise due to incomplete design information. The alternative is the use of physical tests, which are anyway more accurate compared to simulations. In both variants, the tool-tip inertances can be coupled to obtain the accelerations.

The extension of the parametric space should, ideally, contain only the important parameters that might influence chatter apparition. In this regard, detailed sensitivity analyses were carried out for the cutting tool itself and for the workpiece–tool assembly. Based on the results obtained from the analysis reduced only to the assembly, it was concluded that the main parameter of influence for inertances is the rp parameter representing the distance between the tool-tip and workpiece clamping.

Modal behaviors and the influences that various parameters have on accelerance present significant differences depending on the component of the cutting force ($Fn = Fx$; $Ft = Fy$ for longitudinal turning). The experimental determination of these transfer functions is usually done directly on the cutting tool, without the modeling of the workpiece and/or interactions.

To more accurately model the modal behavior of the entire MU, it was decided to develop special system pretensioning devices, with the modeling of the workpiece and with the possibility of measuring the preload forces. Two separate devices were developed for each tested direction, with the design focused on the geometric fidelity of the SVJBL 2020K 16 cutting tool and overcoming the constructive/cinematic constraints found in the tested MU. (CNC PO PY GIM PLG-42).

The original variants were optimized using another complex synergy of parametric exploration, where multiple static and dynamic solutions present in the Siemens SimCenter 3D digital solutions suite were used. The input variables aimed at optimizing the sensitivity of the instrumented areas. The measurement of the preload forces was carried out using strain gauges applied to key areas on the devices, with the development of the hardware and software solution required for the calibration process and use. Calibration was carried out using a single procedure, which allowed the correct orientation and loading of devices using known masses. The linearity of the results confirmed the validity of the procedure.

The measurement of the inertances was done both for the general case, without having the cutting tool in contact with the workpiece, and for the case where the preloading devices are applied. Sensors developed by the PCB company were used, including the impact hammer, with data acquisition and processing solutions developed by Siemens. (Siemens TestLab). The main objective in this phase of the research was to map the dynamic state of the tool-tip (inertances) according to the geometric and functional parameters targeted by each test case, these being coupled with the spectra of the cutting forces determined in the first part of the work. Critical behaviors correlated with variation in the parameters investigated for both configurations were identified, confirming the need to extend the parametric space used to generate the training samples. In this phase of the research, it was also possible to compare the simulated results with those obtained from measurements, their interpretation validating the concept's ability to capture complex dynamic behaviors even when using reduced modeling of the generator system.

A noticeable, anticipated, important feature for both cases is the difference in the complexity of the dynamic response according to the direction. The variation of complexity in the $Fx$ direction is much greater compared to the variation in the $Fy$ direction. This aspect drastically influences the structure and defining parameters of the AI solution, suggesting that this might be important for future researchers.

The key component of the fundamental concept proposed in this PhD thesis is the validation of the applicability of AI technologies in order to estimate the unwanted dynamic behavior of the machine tools. Exposure to this feature was experimentally achieved by testing several models of neural networks with different structures and training parameters. As expected, the high degree of complexity of the variation of modal characteristics on the $Fx$ direction greatly complicates the process of determining the most efficient drive variant, with substantial costs on computational performance. At the same time, it was confirmed that for this application there is no standard approach that can be used in the construction of AI solutions, the exotic behaviors obtained attest to the volatile feature of the technology which can be interpreted both negatively, by the difficulty of obtaining desired results, and positively by the high degree of flexibility.

# 5 FINAL CONCLUSIONS. ORIGINAL CONTRIBUTIONS. DISSEMINATION OF RESEARCH RESULTS. FUTURE RESEARCH

## 5.1 General conclusions

The doctoral thesis focused on the conduct of thorough theoretical and experimental studies on the basis of which innovative concepts with real-life applications were developed in the active control of dynamic phenomena in cutting processes, using artificial intelligence. The work proposes, tests and validates innovative methods, numerical models and experimental prototypes in a synergistic context, enabling the realization of a generic platform for the implementation of these technologies across a wide range of machine-tool and manufacturing processes.

The doctoral thesis is structured in three parts. The first part of the work deals in detail with the current state of the mathematical apparatus and technologies that allow the analysis of dynamic phenomena in machining. Based on the findings of this investigation, it is decided to evaluate the current state of the methods for detecting and controlling the phenomenon of chatter. The results of the investigations showed a high degree of difficulty in understanding, modeling, measuring and controlling this phenomenon, and the findings directly contributed to the development of the solution proposed in the third part of the paper. Multiple research and experiments conducted allow us to formulate conclusions as follows:

I. The analysis of dynamic phenomena in cutting processes involves the separate assessment of the fundamental mechanical components such as modal behavior, friction influence and self-generating phenomenon, the modal component being regarded as independent of the rest;
II. Existing methods of vibration control in cutting operations involve, in the first phase, the detection of negative behaviors. Quantification of the phenomenon is carried out using a wide range of sensors and methods, the achievement of control being directed by techniques of varying degrees of complexity. From this analysis, it was concluded that an active control system with artificial intelligence would adopt an operating scheme similar to those present in reaction loop models, a reaction monitored by means of 'agents';
III. The studies presented in the third part of the thesis were focusing strictly on the design, implementation and testing of all the components involved in the realization of the system development platform proposed. The main aspects pursued in this part were:
    a. Definition of constructive and control parameters to neural networks;
    b. Presentation of the pre/post-processing components needed in the implementation of solutions for active control of the chatter phenomenon based on the latest specialist work;

c. Defining the concept of the training sample, exposing the problems of computational efficiency when using oblique simulations;
d. Developing an innovative solution to reduce the computational cost of simulating cutting processes, while ensuring the scalability of the proposed solution;
e. Introduction of modern methods of parametric exploration with the aim of streamlining the number of simulations necessary to highlight parametric interdependencies;
f. Progressive evaluation of the generating system with a view to showing the parameters that may induce substantial changes in the modal characteristics;
g. Design and optimization of systems for measuring the accelerance of the tool-tip with the application of preload forces;
h. Instrumentation and calibration of measurement prototypes;
i. Conducting experimental tests:
    i. focused on determining the transfer functions of the generator system with the SVJBL 2020K 16 cutting tool as reference;
    ii. focused on determining the transfer functions (accelerance) of the generator system with workpiece modeling and preload;
j. Coupling simulated and measured accelerances with the spectral of cutting forces for comparison purposes;
k. Construction, training and testing AI solutions, evaluating the performance and critical parameters.

Based on the conclusions formulated and the experiments, a general conclusion can be formulated that proves the capability, flexibility, scalability and performance of the proposed methodology in the implementation of AI systems to cutting operations control processes. Consequently, it can be stated that the main objectives of the doctoral thesis have been achieved through the proposed development platform.

## 5.2 Original contributions

The originality of this doctoral thesis is guaranteed by the innovative nature that all the methods, structures and constructive solutions present. In short, personal contributions can be summarized as follows:

- Presentation of the current state of the art in terms of the analysis the dynamic phenomena in cutting operations based on the latast literature;
- Presentation of the current state of worldwide achievements in the active control of chatter phenomena in machine tools;
- Exposing the difficulties of implementing artificial intelligence (AI) technologies on machine tools for the purpose of controlling dynamic phenomena;

- Proposing a new, innovative method of generating synthetic spectral samples for cutting forces using advanced simulation methods (Deform 3D, AdvantEdge). In this context, a new solution has been developed to reduce the complexity of the numerical model, applicable to most cutting operations;
- Combining the cutting operation simulations methods with advanced parametric exploration techniques (Siemens HEEDS MDO), with further optimization of this new method of generating synthetic data through a computational relationship (4.6) adapting the minimum required length of the simulated dislocated chip;
- Exposure the interdependence relationships of cutting regime parameters with direct influence on the distribution of vibrations in the frequency spectrum (Siemens HEEDS MDO);
- Proposing a new method for monitoring the wear of the cutting tool using the simulated dynamic signatures of the system in the AI context (Siemens HEEDS MDO);
- Reproduction of the SVJBL 2020K 16 cutting tool model using the Siemens NX CAD solution, converting it into a numerical model for the purpose of performing complex modal analysis, combining Siemens SimCenter 3D finite element analysis software solution with Siemens HEEDS MDO parametric exploration solution;
- Construction of numerical parametric model describing longitudinal turning. Conducting a complex modal analysis using the same suite of software solutions exposing the main parameters with high potential of influence on dynamic behavior;
- Designing and building two special devices used for measuring the accelerances of the tool-tip for the longitudinal turning operation on the PO PY GIM PLG-42 CNC lathe;
- Development of a complex device optimization solution using a unique structure consisting of finite-element analyses based on the Siemens SimCenter 3D solution, in combination with Siemens HEEDS MDO parametric exploration solution and special heuristics.
- Development of hardware and software elements used to quantify the pre-load level of the devices using BF350 – 3AA gauges, specialized modules ADC HX711 and the Arduino Uno R3 development board;
- Development and execution of calibration procedures of devices developed for the purpose of measuring the accelerances of the tool-point, taking into account the quasistatic preload forces generated by the cutting process;
- Mapping the accelerances of the SVJBL 2020K 16 cutting tool on the PO PY GIM PLG-42 CNC lathe using PCB 333B30 acceleromentre along with the PCB 086C03 impact hammer, Siemens SCADAS XS acquisition system and Siemens TestLab post-processing software solution;
- Analysis the results obtained when measuring the inertances of the SVJBL 2020K 16 cutting tool with the presentation of the main influence parameters and the degree of correlation;

- Measurement of the accelerances of the tool-tip mounted on the PO PY GIM PLG-42 CNC lathe using the specially developed prototypes. Interpretation of results with presentation of the degree of correlation of the results with the simulated results and the parameters affecting the dynamic behavior. The same sensory and acquisition systems were used;
- Coupling the inertance spectrums with the cutting forces in order to obtain final accelerations, presumably measurable in the case of a real application. Comparison of simulation results with hybrid results by combining measured accelerance with the spectrum of simulated cutting forces;
- Implementation of the neural network generation program/module for the purpose of testing proposed implementation assumptions;
- Intensive testing of different neural network configurations and training parameters showing the degree of accuracy depending on computational cost and the behavior complexity.

## 5.3 Future research

The subject of this doctoral thesis is complex. The proposed innovative elements and the results obtained are a contribution to the application of artificial intelligence technologies to the monitoring and control of manufacturing processes. Based on the concepts explored and the results obtained, several future development directions can be formulated such as:

- $loc$ parameter optimization – total length of the chip dislocated in the simulation using heuristics based on the angle of the shear plane, determined analytically;
- Determination of MU transfer functions at the tool and workpiece clamping points in order to replace the ideal rigid boundary conditions applied in the finite element analyses used; confirmation of improved correlations;
- Developing a generic software solution for calibration of preloading devices used to measure tool-tip inertances;
- Expanding the parametric space used to validate the predictive performance of neural networks by adding cutting regime parameters;
- Exploring/testing other types/structures of neural networks with other constructive and control parameters of the training process.

## 5.4 Dissemination of the research results

The results of the research carried out in the context of the present thes were capitalized over time by:

- ✓ publication of 4 scientific papers at international journals/conferences, 3 as first author and 1 in collaboration. Two papers are indexed in Web of Science and three in Scopus.
- ✓ by making available source codes, obtained databases and measurement prototypes to be tested and/or extended for the purpose of developing other similar platforms.

# REFERENCES (extract)

[27] C. Yue, H. Gao, X. Liu, S. Y. Liang și L. Wang, „A review of chatter vibration research in milling," *Chinese Journal of Aeronautics,* vol. 32, nr. 2, pp. 215-242, 2019.

[28] A. Wang, W. Jin, W. Chen, R. Feng și C. Xu, „Bifurcation and chaotic vibration of frictional chatter in turning process," Advances in Mechanical Engineering, vol. 10, nr. 4, 2018.

[29] X. J. Zhang, C. H. Xiong, Y. Ding, M. J. Feng și Y. L. Xiong, „Milling stability analysis with simultaneously considering the structural mode coupling effect and regenerative effect," International Journal of Machine Tools and Manufacture, vol. 53, nr. 1, pp. 127-140, 2012.

[88] B. B. Muhammad, M. Wan, J. Feng și W. H. Zhang, „Dynamic damping of machining vibration: a review," The International Journal of Advanced Manufacturing Technology, vol. 89, pp. 2935-2952, 2017.

[89] E. Kuljanic, G. Totis și M. Sortino, „Development of an intelligent multisensor chatter detection system in milling," Mechanical Systems and Signal Processing, vol. 23, nr. 5, pp. 1704-1718, 2009.

[90] G. Quintana și J. Ciurana, „Chatter in machining processes: A review," International Journal of Machine Tools and Manufacture, vol. 51, nr. 5, pp. 363-376, 2011.

[96] C. A. K. A. Kounta, L. Arnaud, B. Kamsu-Foguem și F. Tangara, „Review of AI-based methods for chatter detection in machining based on bibliometric analysis," The International Journal of Advanced Manufacturing Technology, vol. 122, pp. 2161-2186, 2022.

**[37] A. I. Berariu, I. M. Prodan, C. I. Nită și T. I. Deaconescu, „ANN Samples Generation Using 2D Dynamic FEM for Predicting Machining Vibrations," Acoustics and Vibration of Mechanical Structures—AVMS 2019, vol. 251, pp. 383-393, 2020.**

**[41] A. I. Berariu, I. M. Prodan, C. I. Nită, S. S. Gorobievschi și T. I. Deaconescu, „Cutting dynamics sample generator for artificial neural networks based on design space exploration and explicit simulation synergy," Materials Today: Proceedings, vol. 45, nr. 5, pp. 4189-4195, 2021.**

[102] Wikipedia, „Kriging," 21 10 2022. [Interactiv]. Available: https://en.wikipedia.org/wiki/Kriging. [Accesat 20 01 2023].